Origin of β-Carotene-Rich Plastoglobuli in *Dunaliella bardawil*[1][C][W][OPEN]

Lital Davidi, Eyal Shimoni, Inna Khozin-Goldberg, Ada Zamir, and Uri Pick*

Departments of Biological Chemistry (L.D., A.Z., U.P.) and Chemical Research Support (E.S.), The Weizmann Institute of Science, Rehovot 76100, Israel; and Microalgal Biotechnology Laboratory, French Associates Institute for Agriculture and Biotechnology of Drylands, Jacob Blaustein Institutes for Desert Research, Ben-Gurion University of the Negev, Sede Boker Campus, Sede Boker 84990, Israel (I.K.-G.)

The halotolerant microalgae *Dunaliella bardawil* accumulates under nitrogen deprivation two types of lipid droplets: plastoglobuli rich in β-carotene (βC-plastoglobuli) and cytoplasmatic lipid droplets (CLDs). We describe the isolation, composition, and origin of these lipid droplets. Plastoglobuli contain β-carotene, phytoene, and galactolipids missing in CLDs. The two preparations contain different lipid-associated proteins: major lipid droplet protein in CLD and the Prorich carotene globule protein in βC-plastoglobuli. The compositions of triglyceride (TAG) molecular species, total fatty acids, and *sn*-1+3 and *sn*-2 positions in the two lipid pools are similar, except for a small increase in palmitic acid in plastoglobuli, suggesting a common origin. The formation of CLD TAG precedes that of βC-plastoglobuli, reaching a maximum after 48 h of nitrogen deprivation and then decreasing. Palmitic acid incorporation kinetics indicated that, at early stages of nitrogen deprivation, CLD TAG is synthesized mostly from newly formed fatty acids, whereas in βC-plastoglobuli, a large part of TAG is produced from fatty acids of preformed membrane lipids. Electron microscopic analyses revealed that CLDs adhere to chloroplast envelope membranes concomitant with appearance of small βC-plastoglobuli within the chloroplast. Based on these results, we propose that CLDs in *D. bardawil* are produced in the endoplasmatic reticulum, whereas βC-plastoglobuli are made, in part, from hydrolysis of chloroplast membrane lipids and in part, by a continual transfer of TAG or fatty acids derived from CLD.

Eukaryotic cells accumulate neutral lipids in different tissues mainly in the form of lipid droplets (Murphy, 2012). Most lipid droplets consist of a core of triglycerides (TAGs) and/or sterol esters coated by a phospholipids monolayer and embedded with proteins (Zweytick et al., 2000). Plants accumulate TAGs in different tissues, primarily in seeds but also in fruit, such as palm oil, flowers, and leaves. The best characterized system for TAG metabolism is oil seeds, in which TAG serves as the major carbon and energy reservoir to be used during germination (Huang, 1992, 1996). Recent studies show that lipid droplets are not just static pools of lipids but have diverse metabolic functions (Farese and Walther, 2009). In addition, plants also contain plastoglobuli, small chloroplastic lipid droplets consisting primarily of storage lipids and pigments. Proteome analyses of plastoglobuli suggest that they are involved in synthesis and degradation of lipids, pigments, and coenzymes (Ytterberg et al., 2006; Lundquist et al., 2012). It has been shown that plant plastoglobuli are associated with thylakoid membranes (Austin et al., 2006; Ytterberg et al., 2006).

It is not entirely clear where the TAGs are synthesized in the plant cell. Until recently, it has been assumed that most TAGs are made in the endoplasmatic reticulum (ER) from fatty acids, which are mostly synthesized in the chloroplast and imported to the cytoplasm (Joyard et al., 2010). However, the recent identification of the enzyme diacylglycerol acyl transferase in plant plastoglobuli (Lundquist et al., 2012) suggests that TAG may be synthesized directly in chloroplasts, although direct evidence is missing. TAG may be synthesized also from galactolipid fatty acids during stress or senescence by phytyl ester synthases, which catalyze acyl transesterification from galactolipids to TAGs (Lippold et al., 2012). Phosphatidyl choline (PC) plays a major role in acyl transfer of newly synthesized fatty acids from the chloroplast into TAGs at the ER in plants (Bates et al., 2009). An indication for the origin of glycerolipids in plants is the identity of the fatty acids at the *sn*-2 position: if it originates in the chloroplast, it is mostly C16:0, whereas if it was made in the ER, it is mostly C:18 (Heinz and Roughan, 1983).

Many species of unicellular microalgae can accumulate large amounts of TAGs under growth-limiting conditions, such as nitrogen deprivation (Shifrin and Chisholm, 1981; Roessler, 1990; Avron and Ben-Amotz,

[1] This work was supported by the Alternative Energy Research Initiative Fund at The Weizmann Institute by The Minerva Center: Photosynthesis under stress.

* Address correspondence to Uri.pick@weizmann.ac.il.

The author responsible for distribution of materials integral to the findings presented in this article in accordance with the policy described in the Instructions for Authors (www.plantphysiol.org) is: Uri Pick (Uri.pick@weizmann.ac.il).

[C] Some figures in this article are displayed in color online but in black and white in the print edition.

[W] The online version of this article contains Web-only data.

[OPEN] Articles can be viewed online without a subscription.

www.plantphysiol.org/cgi/doi/10.1104/pp.113.235119

1992; Thompson, 1996). In green microalgae (Chlorophyceae), TAGs are usually synthesized and accumulated in cytoplasmatic lipid droplets (CLDs; Murphy, 2012), although in some cases, such as in *Chlamydomonas reinhardtii* starchless mutants, they also accumulate in chloroplasts (Fan et al., 2011; Goodson et al., 2011). Recent studies indicate that the CLDs are closely associated with ER membranes and possibly, chloroplast envelope membranes as well (Goodson et al., 2011; Peled et al., 2012).

Green microalgae also contain two distinct types of chloroplastic lipid droplets. The first type is plastoglobuli, similar in morphology to higher plants plastoglobuli (Bréhélin et al., 2007; Kessler and Vidi, 2007). The second type is the eyespot (stigma), part of the visual system in microalgae. The eyespot is composed of a cluster of β-carotene-containing lipid droplets organized in several layers between grana membranes in the chloroplast (Häder and Lebert, 2009; Kreimer, 2009). Recent proteomic analysis of algal eyespot proteins revealed that they contain diverse structural proteins, lipid and carotenoid metabolizing enzymes, transporters, and signal transduction components (Schmidt et al., 2006).

The origin of TAG in microalgae is still not clear. In *C. reinhardtii*, it was found that the major fatty acids in the *sn*-2 position are 16:0, which according to the plant dogma, is made in the chloroplast (Fan et al., 2011). In *C. reinhardtii*, which lacks PC, monogalactosyldiacylglycerol (MGDG) was proposed to replace PC in the mobilization of fatty acids from plastidal galactoglycerolipids into TAG based on mutation of a galactoglycerolipid lipase (Li et al., 2012). Based on these results and others, it has been proposed that, in *C. reinhardtii*, triglycerides are primarily produced in the chloroplast or combined with ER (Li et al., 2012; Liu and Benning, 2013).

Plants and algae lipid droplets contain structural major proteins localized at the lipid droplet periphery, and their major function seems to be stabilization and prevention of fusion (Huang, 1992, 1996; Katz et al., 1995; Frandsen et al., 2001; Liu et al., 2009). In plant seed oils, the major classes of lipid droplet proteins are oleosins and caleosins, which have a characteristic hydrophobic loop with a conserved three Pro domain (Hsieh and Huang, 2004; Capuano et al., 2007; Purkrtova et al., 2008; Tzen, 2012). Oleosin and caleosin analogs were also recently identified in some green microalgal species (Lin et al., 2012; Vieler et al., 2012; Huang et al., 2013). However, the most abundant lipid droplets proteins in green algae (Chloropyceae) are a new family of major lipid droplet proteins (MLDPs) structurally distinct from plant oleosins and caleosins (Moellering and Benning, 2010; Peled et al., 2011; Davidi et al., 2012). Plastoglobules have different major lipid-associated proteins termed plastoglobules-associated protein-fibrillins, which form a distinct protein family with no sequence or structural similarities to oleosins (Kim and Huang, 2003). We have previously identified in the plastoglobuli rich in β-carotene (βC-plastoglobuli) a lipid-associated protein termed carotene globule protein (CGP), whose degradation destabilized the lipid droplets (Katz et al., 1995). The proteome of *C. reinhardtii* lipid droplet indicates that algal CLDs also contain several enzymes, suggesting that they are involved in lipid metabolism (Nguyen et al., 2011).

The halotolerant green algae *Dunaliella bardawil* and *Dunaliella salina* 'Teodoresco' are unique in that they accumulate under high light stress or nitrogen deprivation large amounts of plastidic lipid droplets (βC-plastoglobuli), which consist of TAG and two isomers of β-carotene, all trans and 9-cis (Ben-Amotz et al., 1982, 1988). *D. bardawil* also accumulates CLD under the same stress conditions, similar to other green algae (Davidi et al., 2012). It has been shown that the function of βC-plastoglobuli is to protect the photosynthetic system against photoinhibition (Ben-Amotz et al., 1989). The enzymatic pathway for β-carotene synthesis in *D. bardawil* and *D. salina* has been partly identified, but the subcellular localization of β-carotene biosynthesis is not known (Jin and Polle, 2009). The synthesis of β-carotene depends on TAG biosynthesis (Rabbani et al., 1998); however, the origin of βC-plastoglobuli is not known. Are they formed within the chloroplast, or are they made in the cytoplasm? Is the TAG in βC-plastoglobuli and CLD identical or different, and where is it formed?

D. bardawil is an excellent model organism for isolation of lipid droplet for several reasons. First, *D. bardawil* contains large amounts of both CLD and βC-plastoglobuli (Ben-Amotz et al., 1982; Fried et al., 1982), making it possible to obtain sufficient amounts of proteins and lipids from the two types of lipid pools for detailed analyses. Second, *Dunaliella* do not have a rigid cell wall and can be lysed by a gentle osmotic shock, which does not rupture the chloroplast. Therefore, it is possible to sequentially release pure CLD and βC-plastoglobuli by a two-step lysis (Katz et al., 1995). Third, *D. bardawil* seems to lack the eyespot structure, which can be clearly observed in other *Dunaliella* spp. even in a light microscope or by electron microscopy, but has never been observed in *D. bardawil* by us. It avoids the risk of cross contamination of βC-plastoglobuli with eyespot proteins. Fourth, the availability of protein markers for the major lipid droplet-associated proteins, CGPs and MLDPs, enabled both good immunolocalization and careful monitoring of the purity of the preparations by western analysis.

In this work, we describe the purification, lipid compositions, and protein profiles of two lipid pools from *D. bardawil*: CLD and plastidic βC-plastoglobuli. A detailed proteomic analysis of these lipid droplets will be described in another work. Combined with detailed electron microscopy studies, these results led to surprising conclusions regarding the origin of the plastidic βC-plastoglobuli.

RESULTS

Isolation and Lipid Composition of CLD and Plastidic βC-Plastoglobuli from *D. bardawil*

CLD and βC-plastoglobuli were isolated from *D. bardawil* essentially as described earlier (Katz

et al., 1995), with one modification. In brief, cells incubated for 48 h in nitrogen-depleted medium at high light were washed and lyzed by a gentle osmotic shock. We noticed that the osmotic shock does not release most of the CLD from the lyzed cells and therefore, introduced a syringe treatment after osmotic cell disruption, which released the majority of the CLDs as shown by the protein SDS-PAGE profile and the level of TAG in the preparation (Supplemental Fig. S1). Chloroplasts were washed and lyzed by sonication. CLD and βC-plastoglobuli were isolated by flotation centrifugation through Suc density layers. Control cells grown in nitrogen-sufficient medium were also analyzed.

The two populations of purified lipid droplets, CLD and βC-plastoglobuli, were analyzed by Nile red and thin-layer chromatography (TLC). In the Nile red fluorescence staining (Fig. 1A), both CLD and βC-plastoglobuli show the characteristic staining of neutral lipids at 580–590 nm, which is also apparent in intact nitrogen-deprived cells. No chlorophyll fluorescence emission was observed at 685 nm, indicating that the two lipid pools are practically clean of contamination by chloroplast membranes. TLC analysis of neutral lipid composition (Fig. 1B) reveals that CLDs contain mostly TAG, whereas βC-plastoglobuli also contain high amounts of β-carotene and another minor carotenoid. Both preparations also contain small amounts of polar lipids and no detectable chlorophyll. To further analyze the trace polar lipids, larger amounts of total lipid extracts were resolved on TLC, and the samples were compared with thylakoid lipid extracts (Fig. 1C). The polar lipid compositions differ between the two preparations: whereas βC-plastoglobuli polar lipids are almost identical to thylakoid in lipid composition, predominated by MGDG and digalactosyldiacylglycerol, which was confirmed by galactololipid staining (Fig. 1C, Right), the CLDs contain two different polar lipid components that are not galactolipids.

To compare the TAG molecular species of the two droplet populations, we analyzed lipid extracts by reverse-phase HPLC using a Halo-C8 column. The chromatograms of CLD and βC-plastoglobuli lipid extracts are shown in Figure 2. The two chromatograms are very similar, except for three peaks that appear only in the chromatogram for βC-plastoglobuli lipid extracts. Two major peaks (at 5 and 8 min) were identified as β-carotene and phytoene (a β-carotene precursor), respectively, based on their absorption spectra as determined by a diode array detector. The third peak (TAG peak that was collected and sent to mass spectrometry [MS] and fatty acid methyl ester [FAME] analysis; at 33.3 min; Fig. 2) is a unique TAG species that does not appear in other *Dunaliella* spp. Of the major TAG peaks (between 9 and 28 min), each composed of two to three individual components, the minor smaller peaks (between 9 and 17 min) show slight differences in relative peaks distributions, whereas the three major peaks (between 18 and 28 min) are almost identical in both fractions. TAG peaks were identified by reference to TAG standards.

Fatty acid composition analysis of *D. bardawil* cells and the two types of lipid droplets was conducted by gas chromatography (GC) analysis of the FAMEs (Fig. 3A). The two populations of lipid droplets were highly enriched in the fatty acid 18:1ω9 compared with whole-cell extracts, reaching about 40% of the fatty acid content of isolated lipid droplets. In contrast, both populations were relatively deprived of fatty acids 18:3ω3 and 16:4ω3, which are components of the chloroplast thylakoid membrane (Evans et al., 1982). These results are in agreement with our previous study in *D. salina* (Davidi et al., 2012) and studies in *C. reinhardtii*, which showed elevated levels of 18:1ω9, under nitrogen deprivation (Wang et al., 2009; James et al., 2011, Siaut et al., 2011).

As noted above, the identity of the fatty acids at the *sn*-2 position in higher plants is considered as an indicator for its origin: 18C when made in the ER or 16C when made in the chloroplast. To test the applicability of this criterion to *Dunaliella* lipids, we analyzed the fatty acid compositions at the *sn-2* and *sn-1* positions of cytoplasmatic membrane polar lipids (microsomal fraction) and thylakoid membrane galactolipids as controls for ER- and chloroplast-made lipids. Because we found that microsomal lipid extracts contain significant amounts of galactolipids, indicating chloroplast membrane contamination, we performed the positional analysis on isolated PC, which is a component in microsomal membranes but excluded from chloroplast membranes (Supplemental Table S1). The analysis was made by exposure of the isolated PC to phospholipase A2, which specifically cleaves fatty acids at the *sn-2* position, and the thylakoid galactolipids to Rhizopus lipase, which specifically cleaves fatty acids at the *sn*-1+3 position. As expected, galactolipids *sn-2* fatty acids are mostly 16C in length predominated by 16:4, consistent with a chloroplast origin (Cho and Thompson, 1987a, 1987b). Conversely, the microsomal *sn-2* fatty acids of PC are slightly enriched in 18C fatty acids, consistent with a previous report in another *Dunaliella* spp. (Ha and Thompson, 1991). Conversely, the chloroplast membranes *sn-1* fatty acids are composed of a mixture of 16C and 18C fatty acids, whereas PC *sn-1* shows a clear 16C bias, consistent with previous reports (Ha and Thompson, 1991). Next, we analyzed the *sn-1+3* and *sn-2* positions of TAG in CLD and βC-plastoglobuli (Fig. 3, B and C) by exposure of isolated TAG to Rhizopus lipase. As shown in Figure 3C, the fatty acids compositions at the *sn*-2 positions in both lipid pools contain a similar mixture of 16C and 18C fatty acids, with a slight 18C bias for CLD TAG, clearly differing from chloroplast galactolipids (16C/18C = 20; Table I) but resembling microsomal polar lipids. The *sn*-1 +3 position fatty acids in both TAG pools are enriched in 18C fatty acids but differ in the higher level of palmitic acid (16:0) in βC-plastoglobuli.

Time Course of Formation of CLDs and Chloroplastic Lipid Droplets

To learn if the formation of CLD and chloroplastic βC-plastoglobuli occurs simultaneously or if one precedes the other, we performed a physical separation

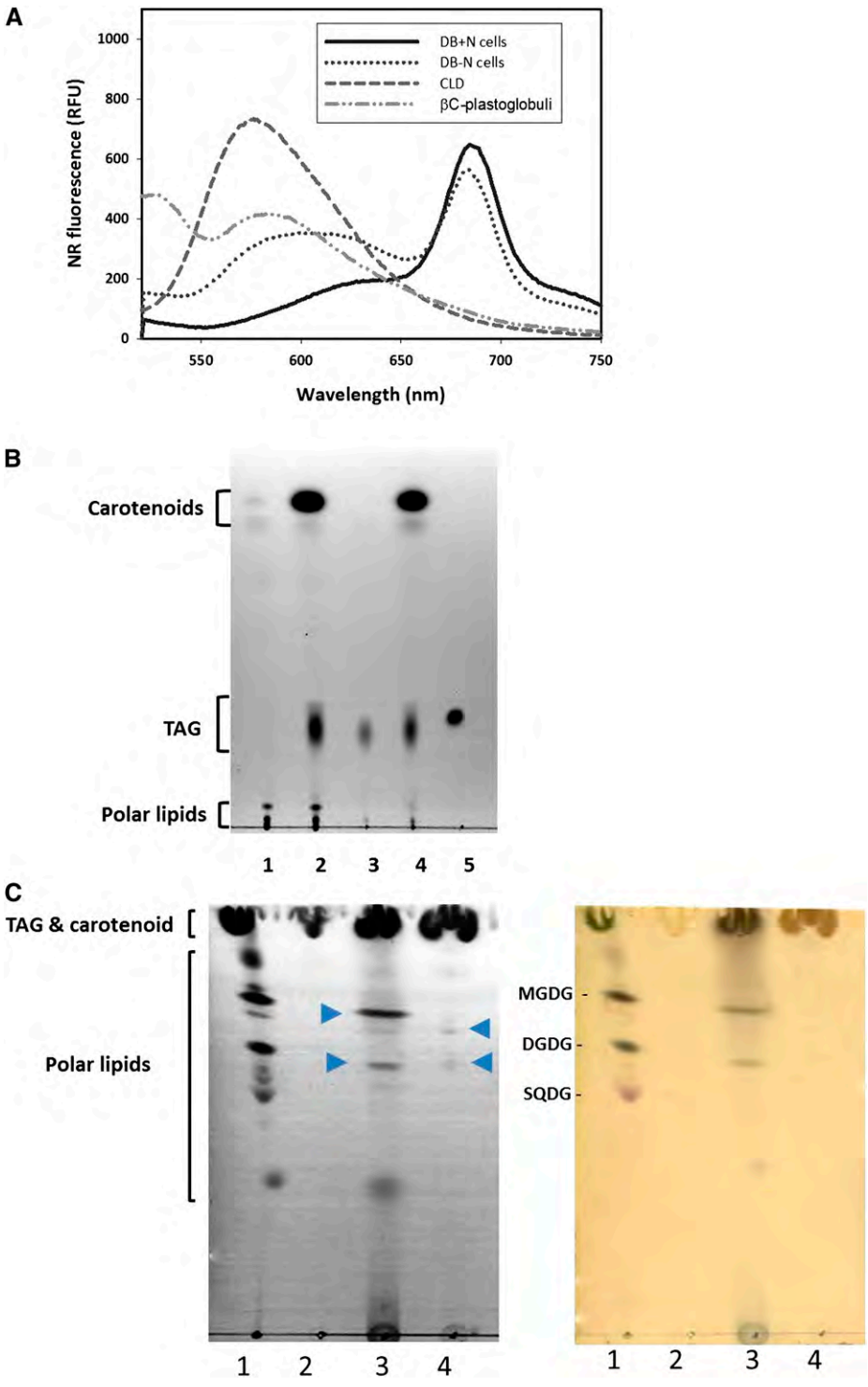

Figure 1. TLC and Nile red analysis of isolated lipid droplets. A, Nile red (NR) fluorescence emission spectra of *D. bardawil* control cells (DB+N), nitrogen-deprived cells (DB-N), and purified CLD and βC-plastoglobuli. B, TLC analysis of neutral lipids in lipid extracts from *D. bardawil* control cells (lane 1), nitrogen-deprived cells (lane 2), purified CLD (lane 3), purified βC-plastoglobuli (lane 4), and 1 μg of triolein standard (lane 5). C, TLC analysis of polar lipids in extracts from *D. bardawil* chloroplasts (lane 1), 1 μg of diacylglyceride standard (lane 2), purified βC-plastoglobuli (lane 3), and purified CLD (lane 4) after iodine staining (Left) and galactolipid staining (Right). The major polar lipids of CLD and βC-plastoglobuli are marked in arrowheads. TLC and Nile red analysis were conducted in samples normalized to equal cell number. DGDG, Digalactosyldiacylglycerol; SQDG, sulfoquinovosyldiacylglycerol. [See online article for color version of this figure.]

and quantitation of the TAG contents of the two lipid populations at different times after exposure to nitrogen deprivation.

As shown in Figure 4A, the rate of TAG accumulation in the two lipid populations is very different: whereas CLDs increase in level until 48 h and then decrease, chloroplastic plastoglobuli increase mostly after 3–6 d. These results suggest that the formation of CLD precedes that of chloroplastic βC-plastoglobuli.

Pulse-labeling experiments with ^{14}C-palmitic acid (^{14}C-PA) were designed to answer three questions. Are TAGs in the two lipid pools synthesized de novo from newly incorporated fatty acids? Are TAGs produced from degradation of membrane polar lipids in the

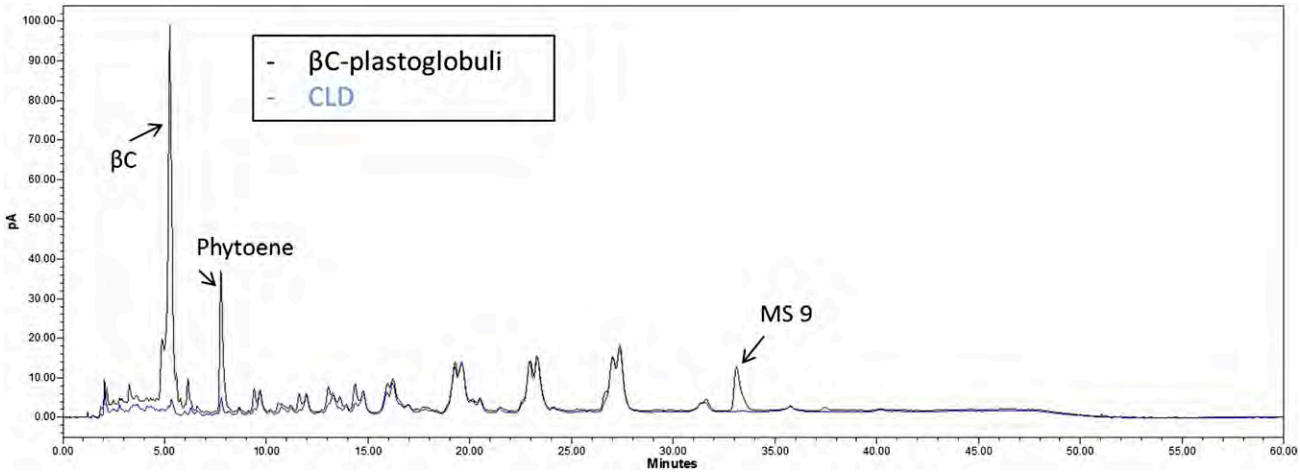

Figure 2. HPLC chromatogram of lipid extracts from cytoplasmic droplets and βC-plastoglobuli. The chromatogram represents lipid extraction fractions from cytoplasmic droplets (blue) and βC-plastoglobuli (black) and was compared with TAG standards. βC, β-Carotene; MS-9, TAG peak that was collected and sent to MS and FAME analysis. [See online article for color version of this figure.]

chloroplast or microsomal cytoplasmic membranes? Are TAGs in βC-plastoglobuli made from preformed TAGs in CLD? ^{14}C-PA was chosen, because we found that this fatty acid, which is a major component in all polar and neutral glycerolipid fractions in *D. bardawil*, is rapidly incorporated into both cytoplasmic and chloroplastic membrane lipids as shown below. To answer the first and third questions, nitrogen-deprived cells were labeled for 4 h with ^{14}C-PA, and then, all free ^{14}C-PA was removed by washing and supplementation of 250-fold excess unlabeled PA. After different periods of incubation in nitrogen-deprived medium, cells were disrupted, and ^{14}C contents in CLD, βC-plastoglobuli, cytoplasmatic microsomal membranes, and chloroplast membranes were analyzed. If βC-plastoglobuli TAGs are produced from CLD TAGs, then we expected to find increased labeling in βC-plastoglobuli correlated with a decreased labeling in CLD.

The ^{14}C distribution pattern (Fig. 4B) showed fast incorporation into both microsomal and chloroplast membranes followed by a decrease with time, indicating that there is no permeability barrier for PA into the chloroplast. The decrease with time in ^{14}C content in the two membrane fractions differs. In microsomal membranes, the decrease continues for 72 h, reaching about 15% from the point of PA dilution, whereas in the chloroplast membranes, ^{14}C decrease levels off after 24 h; it is roughly correlated with the decrease in chlorophyll (Fig. 4C), suggesting that, in the microsomal membranes, the decrease is mostly caused by degradation and resynthesis of new lipids (turnover), whereas in chloroplast membranes, the decrease results from net degradation of about 60% of the membranes and no de novo synthesis.

The time courses of ^{14}C incorporation into the two polar lipid droplets greatly differ; whereas in CLD, there is a 7-fold increase in labeling in the first 24 h followed by a subsequent small decrease, in βC-plastoglobuli, there is a small but progressive increase in labeling during 72 h (Fig. 4B). The large increase in incorporation into CLD in the first 24 h is correlated with the major decrease in labeling of both chloroplast and microsomal membrane lipids, which could indicate acyl editing (namely, that PA is first incorporated into specific polar membrane lipids and next transacylated into TAG; Bates et al., 2009; Li et al., 2012). The subsequent decrease in labeling in CLD between 40 and 88 h of nitrogen deprivation is roughly correlated with the increase in labeling in βC-plastoglobuli (53,000 and 41,000 cpm, respectively).

To test if βC-plastoglobuli TAG may be synthesized from degradation of preformed chloroplast (or other membrane) polar lipids, we designed another ^{14}C-PA pulse-labeling experiment, in which *D. bardawil* cells were incubated with ^{14}C-PA in nitrogen-sufficient (complete) growth medium before entering nitrogen deprivation, and then, residual ^{14}C-PA was removed by washing and dilution with access to unlabeled PA. Samples of cells taken at 0 or 48 h after entering nitrogen deprivation were disrupted and fractionated into membrane and lipid droplets, and their ^{14}C contents were analyzed.

As shown in Figure 5 and Table II, the ^{14}C distribution in CLD and βC-plastoglobuli is very different from the de novo synthesis experiment (Fig. 4B). Over one-third of the total ^{14}C in all lipid fractions was recovered in the βC-plastoglobuli fraction compared with 5% in the de novo synthesis after 40 h, whereas the CLD fraction contained about 20% of the total ^{14}C compared with over 80% in the de novo synthesis experiment. The number of counts recovered from the βC-plastoglobuli fraction was similar to the decrease in counts in the chloroplast membrane fraction

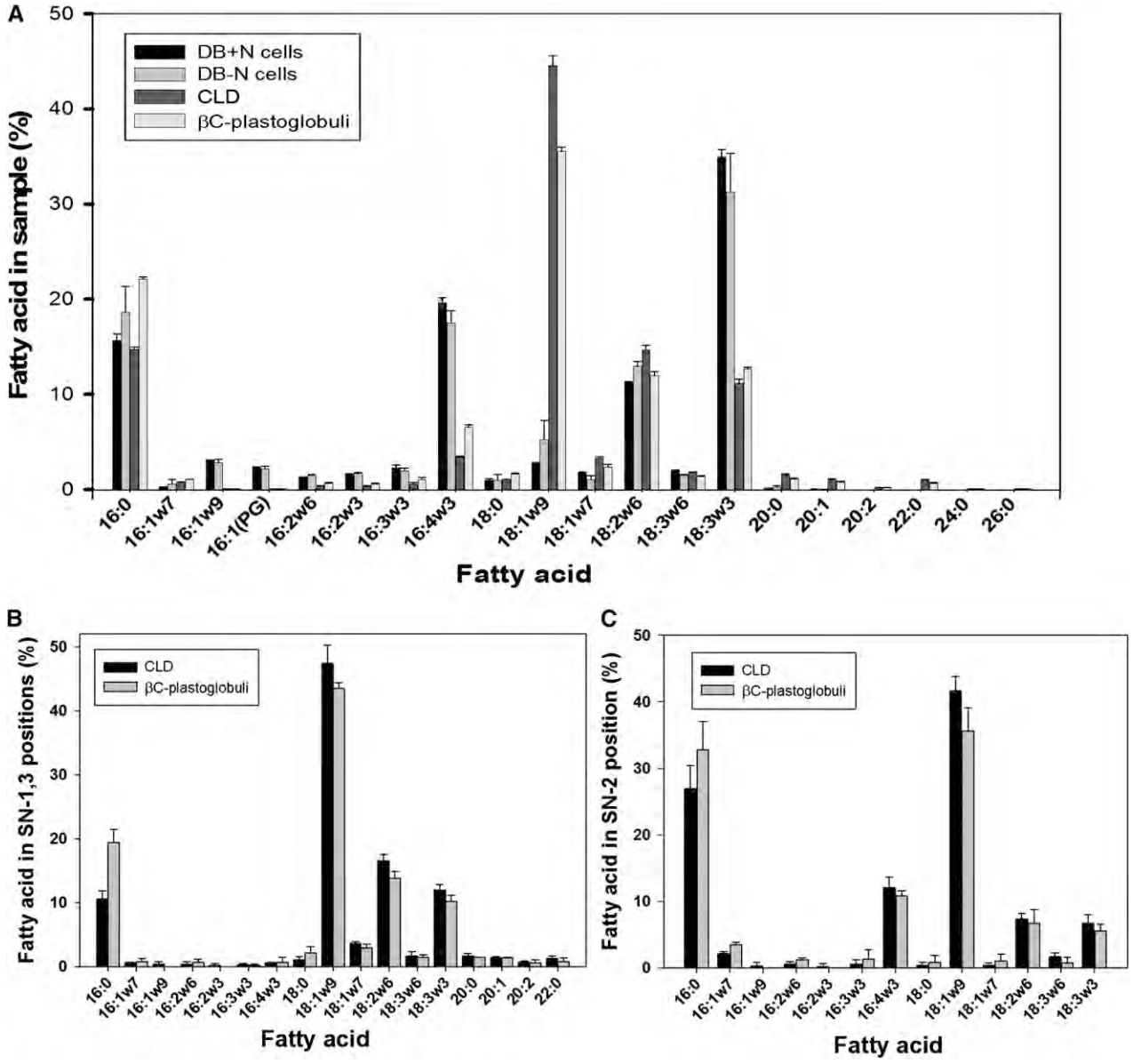

Figure 3. Fatty acid composition and positional analysis of *D. bardawil* isolated lipid droplets. A, Total fatty acid composition analysis of DB+N and DB-N cells together with isolated lipid droplets (CLD and βC-plastoglobuli). Fatty acid compositions of TAG *sn*-1+3 (B) or *sn*-2 (C) positions from CLD and βC-plastoglobuli are shown. The values shown represent means and SDs of three to five replicates.

(285,000 compared with 260,000 cpm, respectively), constituting about 50% of the total 16C fatty acids in polar chloroplast membrane lipids. Also, the recovery of ^{14}C-labeled TAG in CLD was close to 40% of the microsomal ^{14}C content at the onset of nitrogen deprivation, suggesting significant use of 16C fatty acids for production of TAG from degradation of polar membrane lipids in both fractions, particularly of βC-plastoglobuli. The larger decrease in microsomal ^{14}C contents during 48 h of nitrogen deprivation is consistent with the faster lipid turnover in microsomal membranes.

Protein Composition

Protein analysis of the purified droplets was conducted by SDS-PAGE (Fig. 6A). The analysis revealed

Table I. *sn-2 16C/18C fatty acid ratios in different lipid fractions*

The 16C/18C fatty acid ratios were calculated from the fatty acid contents in Figure 3, B and C, and Supplemental Table S1.

Lipid Class	Cytoplasm	Chloroplast
TAG	0.75	1.00
Polar lipids	0.69	17.6

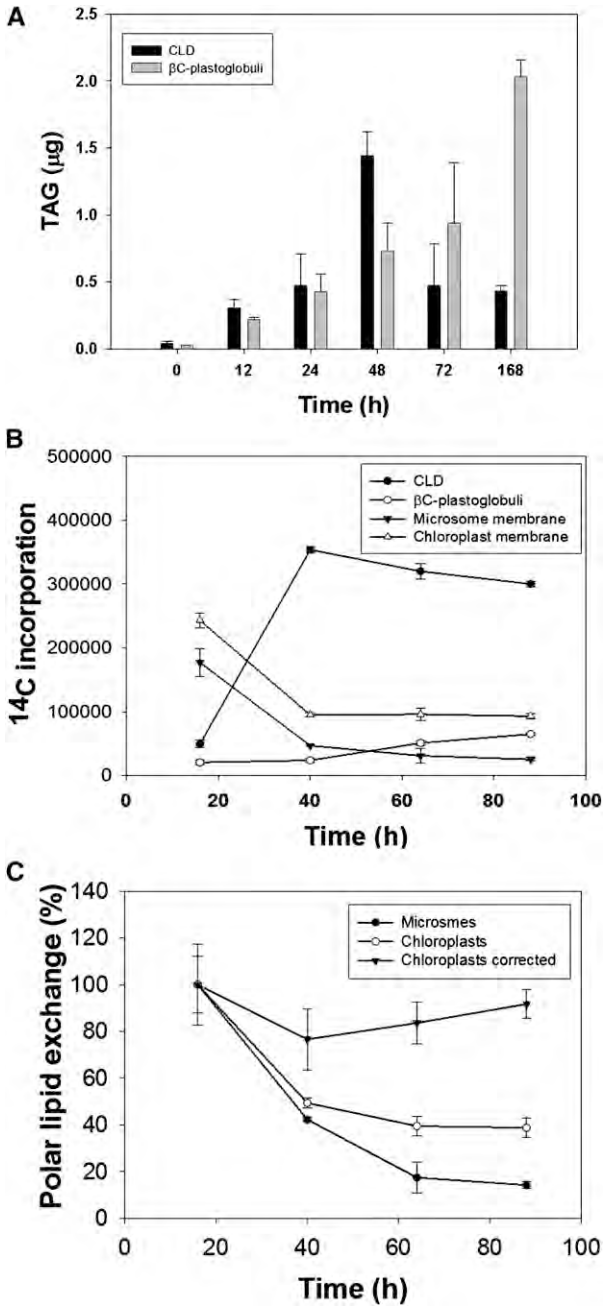

Figure 4. Time course of formation of CLD and βC-plastoglobuli TAG. A, Total TAG contents. *D. bardawil* cells were grown in nitrogen-deficient media. At each indicated time, the cytoplasm and chloroplast fractions were separated, and TAGs were extracted from each fraction. The values shown represent means and SDs of three replicates. B, Incorporation of ^{14}C-PA during nitrogen deprivation into cytoplasmic and chloroplast membranes and lipid droplets. Cells were labeled with ^{14}C-PA for 4 h starting 12 h after the onset of nitrogen deprivation. Cell samples taken at 0, 24, 48, or 72 h after labeling were fractionated, and the ^{14}C in each fraction was determined. Numbers represent averages of three repeats. C, Turnover of polar lipids cytoplasmic and chloroplastic membranes. ^{14}C contents in cytoplasmic and chloroplastic membrane fractions are expressed as percent from 0 time at the end of labeling with ^{14}C-PA. The chloroplast corrected plot shows the ratio of counts divided by chlorophyll contents in the fraction (also expressed as percentage from 0 time).

different protein patterns of the two lipid droplet pools. The cytoplasmatic fraction was enriched with a 30-kD protein, which was identified in our previous study on *Dunalilla* (Davidi et al., 2012) and termed MLDP. The chloroplastic fraction was enriched with a 36- to 38-kD protein(s) composed of at least two components, which was previously characterized in our group (Katz et al., 1995) and termed CGP.

Western-blot analysis of the purified CLD and βC-plastoglobuli with anti-MLDP and anti-CGP antibodies was conducted (Fig. 6B). For this purpose, anti-MLDP- and anti-CGP-specific rabbits polyclonal antibodies were used (Katz et al., 1995; Davidi et al., 2012). The results show the specificity of anti-MLDP antibodies to the CLD and anti-CGP antibodies to the chloroplast βC-plastoglobuli. No cross reaction with anti-Rubisco antibodies, a common chloroplast contaminant, could be detected in the purified lipid droplets proteins (Fig. 6B, row 1), strengthening the conclusion that the two lipid pools are pure.

CGP Structure

CGP has been isolated and cloned in our laboratory (Shoham, 1995), and it was found to be a nuclear-encoded 378-amino acid protein with 42.5 kD. The best prediction for the cleavage site of the transit peptide is after Ala-67, leaving a mature protein of a calculated molecular mass of about 36 kD, close to the estimated molecular mass from SDS-PAGE. Sequence analysis of CGP and MLDP revealed that these two proteins share only very limited sequence homology. The MLDP is part of a unique group of green algal proteins that does not resemble any other known protein (Davidi et al., 2012). CGP is a Prorich protein with 37 Proresidues (Fig. 7A). A comprehensive BLAST search that was carried out in all EST databases

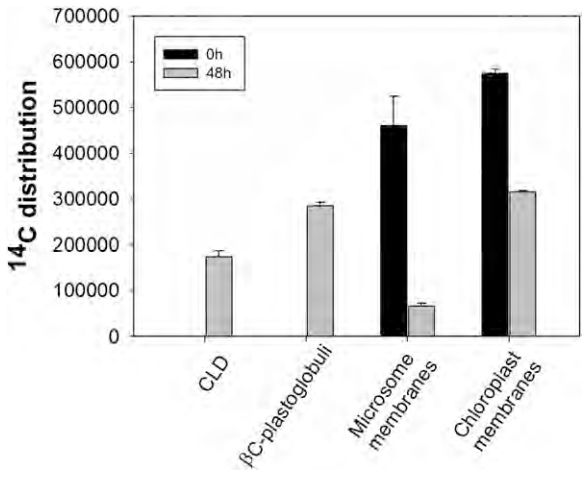

Figure 5. Changes in distribution of ^{14}C-labeled lipids during nitrogen deprivation. Cells were labeled with ^{14}C-PA before the onset of nitrogen deprivation and then deprived of nitrogen for 48 h in the absence of ^{14}C-PA. Black and gray bars represent the levels of ^{14}C in the different lipid fractions before and after nitrogen deprivation, respectively.

Table II. *Comparison of ^{14}C distribution between lipid fractions labeled during nitrogen deprivation or from preformed polar lipids*

A comparison of ^{14}C distribution in lipid fractions in cells labeled during nitrogen deprivation and extracted 24 h after termination of labeling (de novo synthesis, total time at nitrogen deprivation was 40 h; Fig. 4B) or before nitrogen deprivation (synthesis from preformed polar lipids; Fig. 5). The values represent the ^{14}C distribution in each lipid fraction expressed as percentage of total.

Labeling Stage	Nitrogen Deprivation	Prelabeling
	^{14}C Content (% of Total)	
CLD	70.8 ± 1.1	20.8 ± 1.5
βC-Plastoglobuli	4.8 ± 0.6	33.9 ± 1.0
Cytoplasmic membranes	9.4 ± 0.3	7.8 ± 0.8
Chloroplast membranes	15.0 ± 0.7	37.5 ± 0.4

of *D. salina* 'Teodoresco' (GenBank and JGI) identified at least four different CGP genes (Fig. 7B). A BLAST search to CGP in the National Center for Biological Information database of nonredundant proteins identified a low level of homology to SOUL domain-containing proteins (also called SOUL heme-binding proteins). Multiple alignment of CGP with ortholog proteins is available in Supplemental Fig. S2. A phylogenetic tree of algal and Arabidopsis (*Arabidopsis thaliana*) SOUL heme-binding proteins, including CGP, is presented in Figure 7C. MLDP was added to the tree for reference. Notably, SOUL heme-binding proteins are also present in the *C. reinhardtii* eyespot (Schmidt et al., 2006; Wagner et al., 2008) and were detected in Arabidopsis plastoglobules (Ytterberg et al., 2006; Lundquist et al., 2012). Hydropathy plots and Grand average of hydropathy values (GRAVYs) in the work by Kyte and Doolittle (1982; Supplemental Fig. S3A) revealed that CGP and MLDP also differ in their secondary structure: CGP is more hydrophilic (−0.58) compared with MLDP (−0.053). The secondary structure analysis (Guermeur et al., 1999; Supplemental Fig. S3B) shows that MLDP is a highly structured protein, consisting mostly of α-helices, whereas CGP is a mostly unstructured protein, probably because of its high content of Pro residues.

Using software for the prediction of posttranslational modifications revealed no putative conserved sites for palmitoylation, prenylation, myristoylation, or glycosylphosphatidyl-inositol-anchor for the *D. bardawil* MLDP (Davidi et al., 2012), ruling out the possibility of a posttranslational lipid anchor. However, CGP has one predicted palmitoylation site on Cys-13, which probably localizes in the transit peptide.

Cellular Localization of MLDP and CGP

Immunoelectron microscopy was used to determine the cellular localization of MLDP and CGP in *D. bardawil* cells. For the EM analysis, cells were fixed, cryoprotected in Suc, frozen, cryosectioned, and immunolabeled with anti-MLDP or anti-CGP antibody, respectively, followed by gold-conjugated goat anti-rabbit IgG. A comparison of control cells (Fig. 8, A and D) with cells deprived of nitrogen for 6 d shows large accumulation of starch granules and also, lipid droplets in the cytoplasm and chloroplast (Fig. 8, B and E). As shown in Figure 8C and Supplemental Figure S4, MLDP is concentrated at the periphery of the CLD, whereas CGP was localized at the periphery of the chloroplast βC-plastoglobuli (Fig. 8F). Interestingly, MLDP seems to be excluded from the contact area with the chloroplast membrane (Fig. 8C; Supplemental Fig. S4B). No label could be observed in other cellular compartments or control cells. Also, we could not observe labeling of MLDP on βC-plastoglobuli or CGP on the CLD. These results and the western-blot analysis of purified lipid droplets described in Figure 8B justify the use of MLDP and CGP as specific markers for localization of CLD and βC-plastoglobuli, respectively.

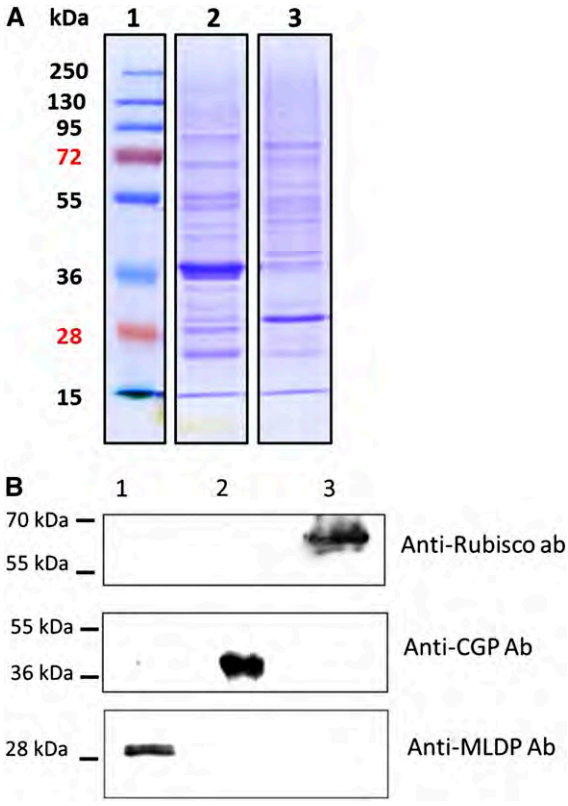

Figure 6. Protein profiles and western-blot analysis of major lipid-associated proteins in CLD and βC-plastoglobuli. A, Protein analysis of CLD and βC-plastoglobuli by SDS-PAGE. Lane 1, Molecular mass standards. Lane 2, Proteins from βC-plastoglobuli. Lane 3, Proteins from CLD. Twenty micrograms of proteins was loaded on each lane. The results shown are representative of three experiments. B, Western blot on purified CLD (lane 1), βC-plastoglobuli (lane 2), and pure chloroplasts (lane 3) proteins with anti-Rubisco (dilution 1:20,000), anti-MLDP (dilution 1:1,000), and anti-CGP (dilution 1:2,000) antibodies (Abs). [See online article for color version of this figure.]

Figure 7. CGP amino acid sequence, paralogs, and phylogenetic tree. A, CGP amino acid sequence. Pro residues are shadowed yellow. Prorich basic domains are marked by lines 1 to 3. The arrow indicates putative cleavage site of the transit peptide. B, Multiple alignment of CGP with three paralogs. C, Phylogenic tree of CGP with SOUL domain proteins from algae and Arabidopsis. The alignment was generated by the CLUSTAL W program, and the phylogram was constructed by the neighbor-joining method using MEGA5 software (Tamura et al., 2011). CGP and orthologs (followed by National Center for Biotechnology Information accession numbers in parentheses): SOUL domain-containing protein (*Coccomyxa subellipsoidea*; EIE18519.1), hypothetical protein (*C. reinhardtii*; XP_001691398.1), hypothetical protein (*Volvox carteri*; XP_002947474.1), predicted protein (*Ostreococcus lucimarinus*; XP_001418356.1), SOUL heme-binding protein (Arabidopsis; NP_001190345.1), hypothetical protein (*Chlorella variabilis*; EFN56543.1), SOUL domain-containing protein in plastoglobules (Arabidopsis; ABG48434.1), and MLDP (*D. bardawil*; AEW43285.1). [See online article for color version of this figure.]

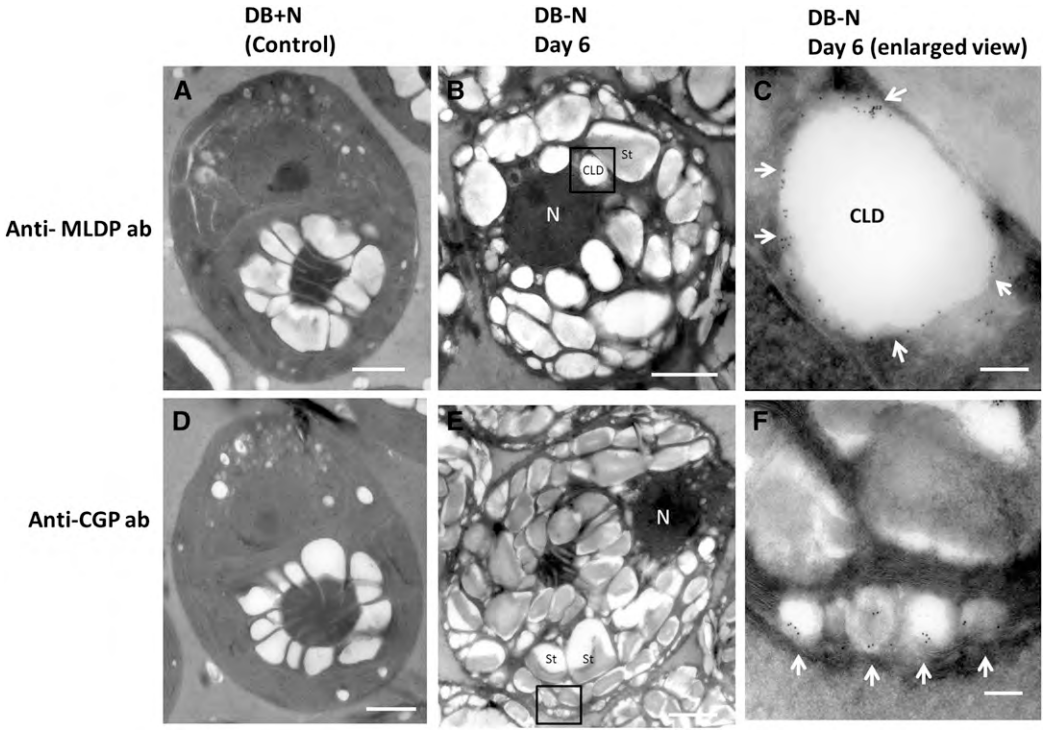

Figure 8. Localization of MLDP and CGP by Gold immunolabeling. Algae were cultured in DB+N or DB-N for 6 d. Cryosections of fixed cells were treated with anti-MLDP or anti-CGP polyclonal rabbit antibodies followed by incubation with 10 nm gold-conjugated goat anti-rabbit antibodies. A, DB+N cells treated with anti-MLDP antibodies. B, DB-N cells treated with anti-MLDP antibodies. C, Enlarged view of B showing high concentration of gold particles (white arrows) in the periphery of the CLD but not in the contact area of the chloroplast. D, DB+N cells treated with anti-CGP antibodies. E, DB-N cells treated with anti-CGP antibodies. F, Enlarged view of E showing gold particles in the periphery of the βC-plastoglobuli (white arrows). N, Nucleus; St, starch. Bars in A, B, D, and E = 2 μm. Bars in C and E = 200 nm.

Time Course of TAG, β-Carotene, CGP, and MLDP Formation

To clarify if the inductions of the proteins CGP and MLDP are correlated with the accumulation of TAG and β-carotene, we followed, in parallel, the mRNA and protein levels of CGP and MLDP, TAG, and β-carotene levels during 7 to 10 d of nitrogen deprivation. *D. bardawil* cells were grown in complete or nitrogen-deprived media for 10 d, and samples for RNA, protein extraction, TAG, and β-carotene were collected at indicated times. Semiquantitative PCR of MLDP and CGP mRNA expression (Fig. 9A) revealed a faster initial expression of MLDP during the first 24 h and maximal protein levels after 4 and 7 d of nitrogen deprivation for MLDP and CGP, respectively (Fig. 9B).

The increases in MLDP and CGP are roughly correlated with the increases in TAG and β-carotene levels, respectively. The accumulation of TAG, determined by TLC analysis, reached maximal level after about 6 d (Fig. 10A), whereas the level of β-carotene increased in two kinetic phases: first, between 0 and 5 d and second, between 6 and 10 d (Fig. 10B). In contrast, control cells did not accumulate either TAG or β-carotene. The chlorophyll content of nitrogen-deprived cells decreased by more than 50% after 4 d of nitrogen deprivation compared with control cells (Fig. 10C).

Origin of Chloroplastic βC-Plastoglobuli as Visualized by Electron Microscopy

Control and nitrogen-deprived *D. bardawil* cells were visualized using different electron microscopy methods. Cryo-scanning electron microscopy (SEM) of control cells (Fig. 11A) reveals oval cells with cup-shaped chloroplasts and small numbers of CLDs. After 2 d of nitrogen deprivation, *D. bardawil* cells increase in size, and the number and diameter of CLDs significantly increase (Fig. 11, B to D). Within the chloroplast, arrays of small βC-plastoglobuli (less than 200 μm in diameter) can also be observed (indicated by white arrows in Fig. 11, C and D).

To monitor the dynamics of CLD and βC-plastoglobuli accumulation during nitrogen deprivation, transmission electron microscopy (TEM) images of *D. bardawil* cells were taken at 0, 1, 3, and 7 d of nitrogen deprivation (Supplemental Figs. S5–S7). To obtain a clearer view of the initial stage of chloroplast βC-plastoglobuli formation, electron tomography

imaging was performed on *D. bardawil* cells after 1 d of nitrogen deprivation (Fig. 12, B to D). Control cells have a highly ordered cup-shaped chloroplast, which occupies most of the cell volume, with small cytoplasmatic intrusions. Hardly any starch or lipid droplets are visible (Fig. 12A). Already after 1 d of nitrogen deprivation, there is a radical change in cell morphology: the chloroplast is filled with starch granules and has fewer thylakoid membranes, and the cytoplasm contains several large lipid droplets of about 500 μm in diameter (Fig. 12B; Supplemental Fig. S5, B to H). Notably, many CLDs seem to be closely associated with the outer chloroplast surface and in some cases, appear almost engulfed by the chloroplast (Supplemental Fig. S5, E and F). Within the chloroplast, arrays of smaller droplets (about 100 μm; marked by red arrows in Supplemental Fig. S5) are bordered by the chloroplast envelope membranes and the outermost thylakoid membranes. In some cases, these small droplets appear tightly squeezed to the large CLD, separated by a nonuniformly stained chloroplast envelope membrane (Fig. 12D). Supplemental Movie S1 of the tomography reconstruction best represents our findings. This morphology was observed in dozens of cells and also seen in cells after 2 and 3 d of nitrogen deprivation, although at a lower frequency (Supplemental Fig. S6). After 7 d of deprivation, the cells appear swollen, and the cytoplasm contains only a few lipid droplets, whereas the chloroplast contains large amounts of starch

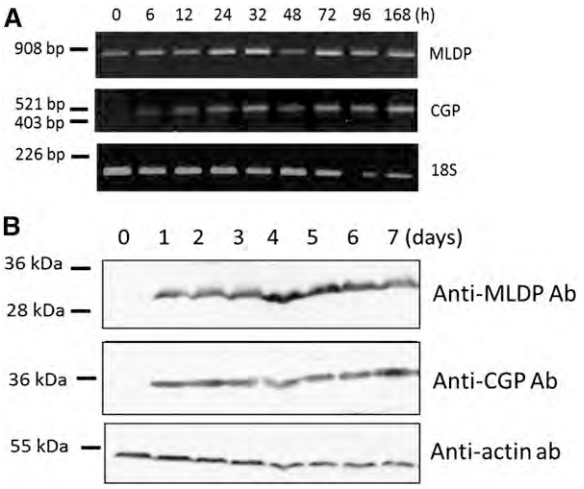

Figure 9. Time courses of mRNA and protein expression of MLDP and CGP. A, mRNA expression of MLDP and CGP. PCR was conducted on complementary DNA (cDNA) extracted from nitrogen-deprived cells at the indicated times with MLDP and CGP complete gene-specific primers, respectively, and 18S primers as control. B, Protein expression of MLDP and CGP was conducted by western-blot analysis. *D. bardawil* was grown in nitrogen-deficient media during 7 d of culturing. Each lane contains proteins extracted from 2×10^6 cells. Dilution of anti-MLDP antibody was 1:1,000 and anti-CGP antibody was 1:2,000. The results shown are representative of three experiments. Ab, Antibody.

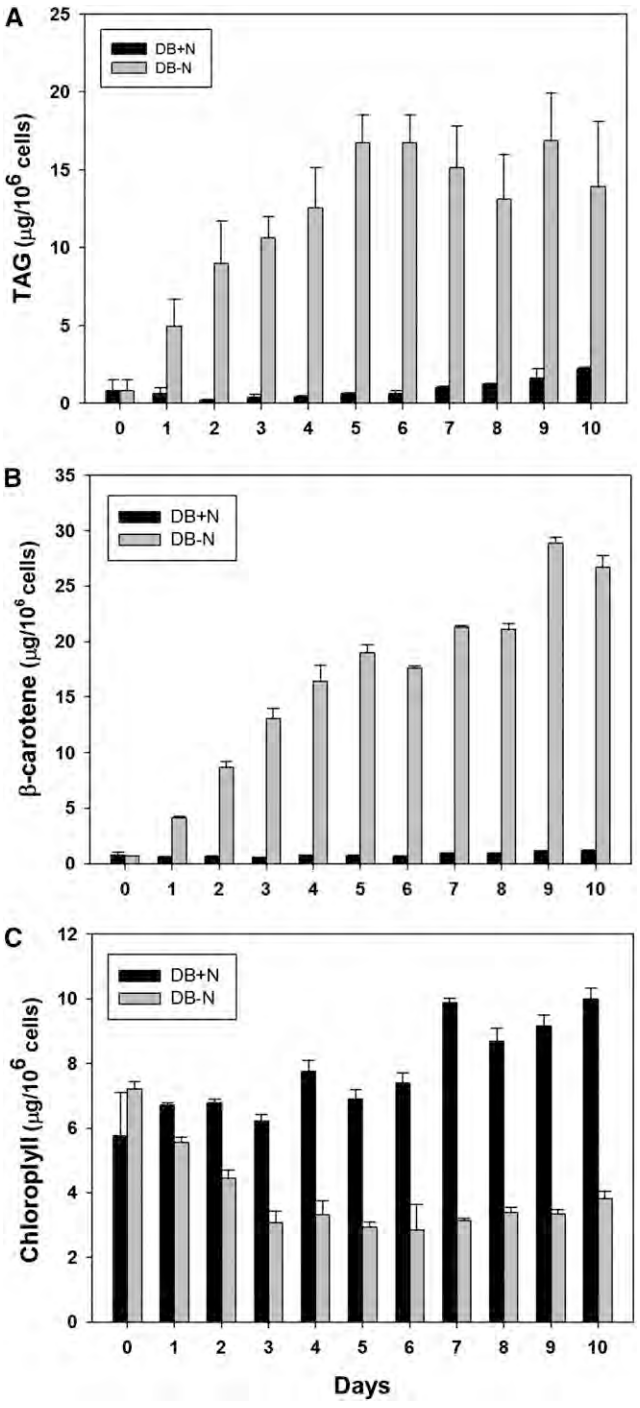

Figure 10. Rates of accumulation of TAG and β-carotene and decrease in chlorophyll during nitrogen deprivation in *D. bardawil*. *D. bardawil* cells were cultured in DB+N or DB-N media for 10 d. A, TAG content of DB+N and DB-N cells. Quantification of TAG by TLC analysis of lipid extracts (Fig. 1B) was by reference to 1 μg of triolein standard. B, β-Carotene content of DB+N and DB-N cells. β-Carotene content was calculated from the absorbance of the cell lipid extracts at 480 nm. C, Chlorophyll content of DB+N and DB-N cells. Chlorophyll content was calculated from the absorbance of the cell lipid extracts at 663 nm. The values shown represent means and SDs of three replicates.

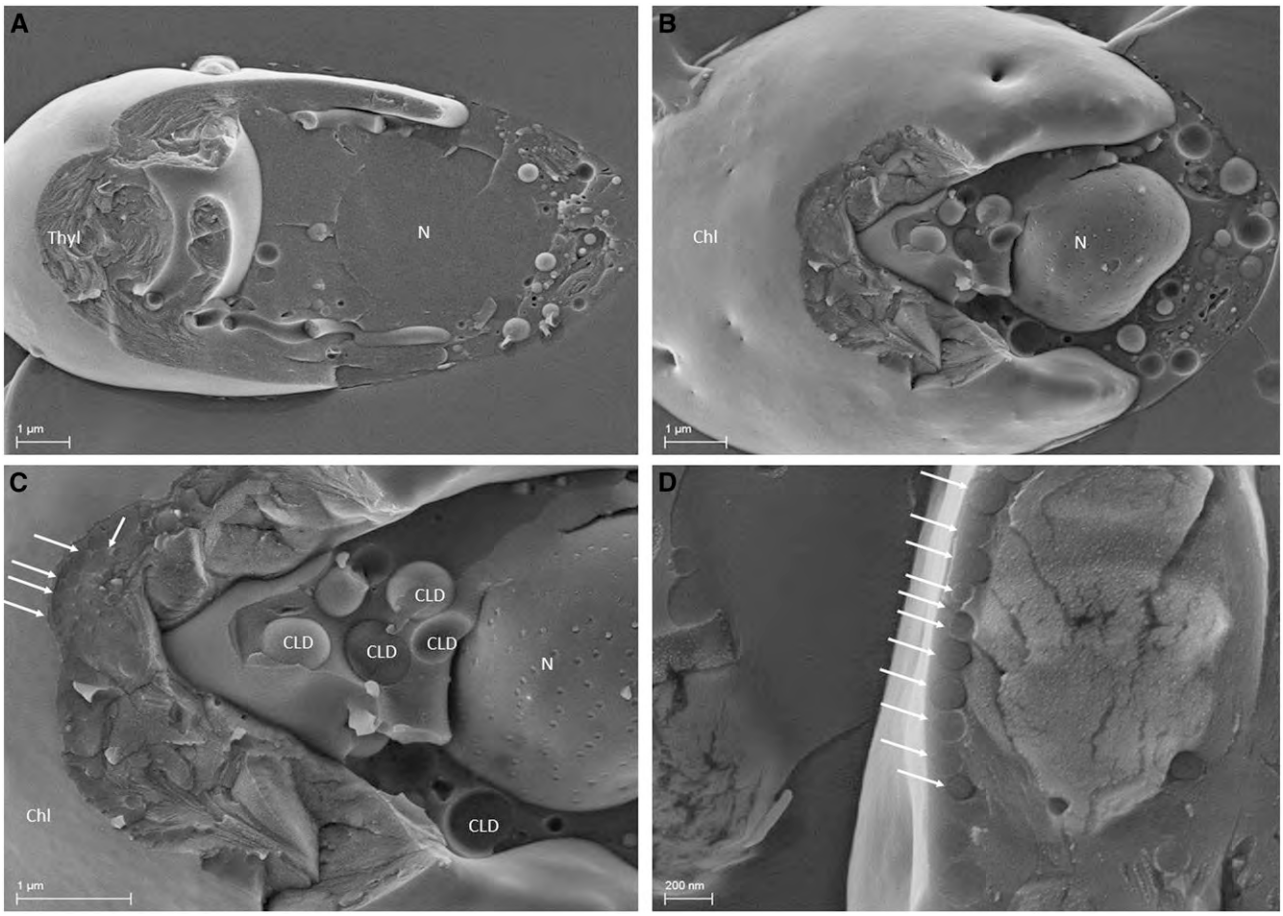

Figure 11. Cryo-SEM images of *D. bardawil* control and nitrogen-deprived cells. A, *D. bardawil* cell grown in complete medium (control cell). B, *D. bardawil* cells after 2 d of nitrogen deprivation. C, Enlarged view of B showing CLD in the cytoplasm and high cluster of βC-plastoglobuli in the chloroplast (white arrows). D, Section of chloroplast showing an array of βC-plastoglobuli (white arrows). Chl, Chloroplast; N, nucleus; Thyl, thylakoid membranes.

granules and a large number of βC-plastoglobuli (ranging in size from 200 to 500 μm) localized mostly at the outer periphery (Supplemental Fig. S7). Some blank spaces and tears to chloroplast membranes in the vicinity of starch granules can be seen, possibly resulting from damage by starch granules during centrifugation.

DISCUSSION

In this work, we tried to clarify the interrelations between two neutral lipid droplets in *D. bardawil*, CLD and βC-plastoglobuli, the latter being unique to this species. It was achieved by improved isolation of the two lipid pools combined with lipid composition analyses, biochemical analyses of lipid biosynthesis, and electron microscopy.

The isolated βC-plastoglobuli and CLD have similar TAG molecular species and fatty acid compositions (total fatty acid and fatty acid at *sn*-1+3 and *sn*-2 positions) but differ in the presence or absence of β-carotene in their polar lipid compositions and their major lipid-associated proteins, which will be detailed below.

A major question that concerned us in this study is the origin of TAG in CLD and βC-plastoglobuli in *D. bardawil*. The finding that TAG *sn-2* fatty acids in both CLD and βC-plastoglobuli are a mixture of 16C and 18C gives no clear indication for a cytoplasmatic origin at the ER, which shows a clear 18C bias in both higher plants (Heinz and Roughan, 1983) and algae, including *Dunaliella* (Ha and Thompson, 1991), or a chloroplastic origin, which has a clear 16C bias (Cho and Thompson, 1987a; Supplemental Table S1), although the cytoplasmatic TAG fatty acid composition is much closer to that of PC than to chloroplast membrane lipids (Table I). A similar *sn-2* fatty acid composition was reported previously for both cytoplasmatic and chloroplast-associated TAGs in *D. salina* (Ha and Thompson, 1991). These results contrast the finding in *C. reinhardtii*, where TAG *sn-2* fatty acids are mostly 16C, indicating that they are made in the chloroplast (Fan et al., 2011). The applicability of the *sn-2* fatty acids

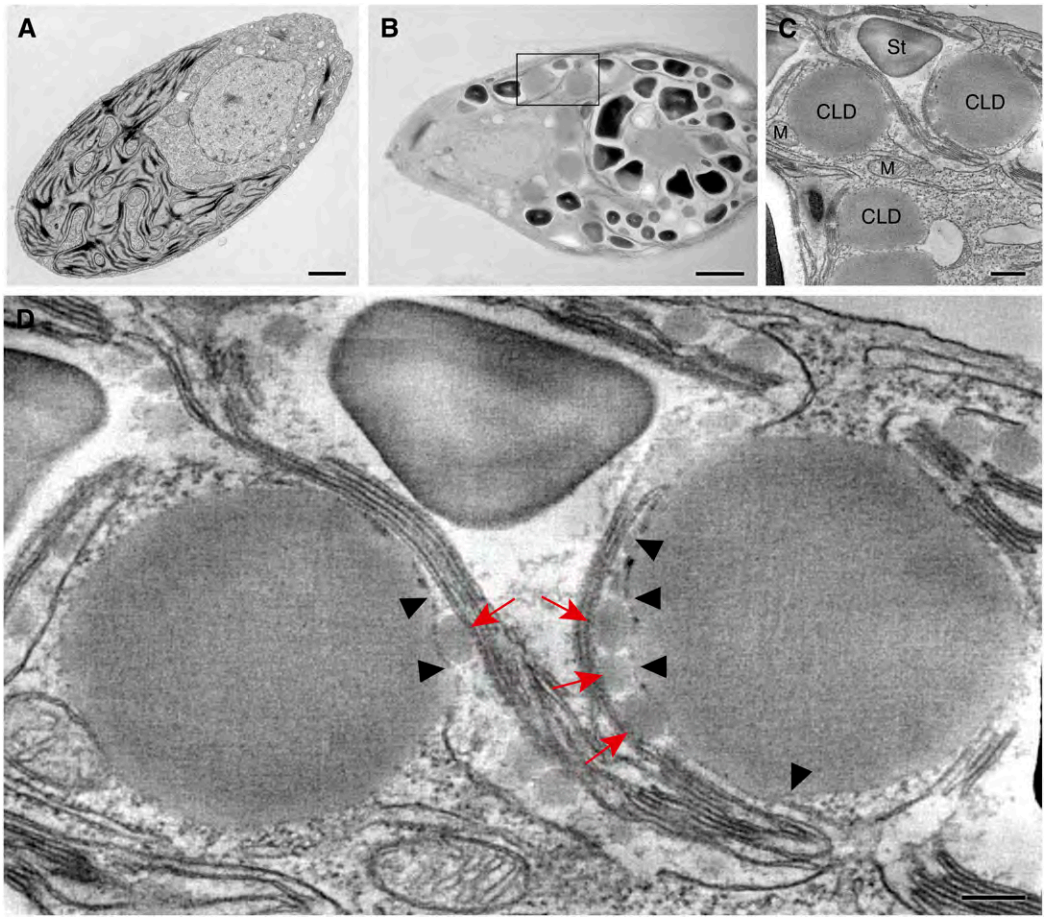

Figure 12. Tomographic reconstruction of *D. bardawil* cell after 1 d of nitrogen deprivation. A, TEM image of control cell grown in nitrogen-sufficient medium. Bar = 1 μm. B, TEM image of cell grown in nitrogen-deficient medium for 1 d. It should be noted that this thick (470-nm) slice was used for tomographic analysis (C and D) compared with the standard 70 nm in A. Bar = 2 μm. C, Tomographic view of a cell section containing four CLD and βC-plastoglobuli. Bar = 500 nm. D, Enlarged view of B showing two CLDs surrounded by a nonuniformly stained chloroplast envelope membranes (arrowheads) and adjacent βC-plastoglobuli (red arrows). Bar = 200 nm. M, Mitochondrion; N, nucleus; P, pyranoid; St, starch. [See online article for color version of this figure.]

criterion for the origin of TAG is questionable, because it is now well-established that the transfer of fatty acid acyl groups into TAG proceeds through acyl editing by specific enzymes with different fatty acid specificities. For example, in *C. reinhardtii*, fatty acid acyl transfer from MGDG to TAG, which has a preference for *sn-1* 18:1 fatty acids (Li et al., 2012), may not alter *sn-2* fatty acid in TAG, whereas PC editing shows a different fatty acid specificity (Bates et al., 2009); phytyl ester synthase1 (PES1) and PES2, which catalyze hydrolysis of fatty acids from chloroplast membrane lipids and their transacylation to TAG (Lippold et al., 2012), show poor specificity for fatty acids and may scramble *sn-2* fatty acid composition in TAG. The finding that PA incorporation into polar lipids precedes the incorporation into TAG (Fig. 4B) suggests that acyl editing is probably part of TAG biosynthesis also in *D. bardawil*.

The origin of TAG in *D. bardawil* lipid droplets is not clear. The very similar fatty acid composition (Fig. 3) and the similar TAG molecular species (Fig. 2), strongly suggest a common origin. In contrast, according to the ^{14}C-PA pulse-labeling experiments, the two TAG pools seem to have different origins. In the first 40–48 h of nitrogen deprivation, most CLD TAG seems to be produced by direct incorporation of newly synthesized fatty acids (Fig. 4B), and a smaller part is from preformed polar lipids (Fig. 5), whereas for βC-plastoglobuli TAG, a significant part of fatty acids, amounting to 50% of 16C fatty acids in chloroplast membranes, seems to be released from degraded chloroplast membrane polar lipids (Fig. 5; Table II). However, chloroplast membrane lipids degradation cannot provide most TAG fatty acids simply because the amount of total membrane fatty acid contents in *D. bardawil* is only around 20% of that of the fatty acid TAG content (for example, Fig. 1B, lane 2).

The only difference in fatty acid composition between the two TAG pools is the higher contents of 16:0 fatty

acids in βC-plastoglobuli, particularly at the *sn1+3* position (Fig. 3). Also, the only significant differences in the TAG molecular species compositions in the two lipid pools are in the low M_r species, which are enriched in 16C fatty acids (peaks between 9 and 17 min; Fig. 2). The reason for these differences may be the higher contribution of 16C fatty acids derived from degradation of chloroplast membrane lipids and incorporated into TAG in plastoglobules, consistent with the ^{14}C-PA pulse-labeling experiments (Fig. 5; Table II) during the first 48 h of nitrogen deprivation.

The time course of TAG accumulation in the two lipid pools and the ^{14}C-PA pulse-labeling experiments (Fig. 4, A and B) suggest that the major biosynthesis of CLD takes place in the first 48 h of nitrogen deprivation/high light stress, whereas the accumulation of βC-plastoglobuli continues for 7 d. Similarly, EM pictures revealed a progressive increase in plastoblobuli and a decrease in CLD from day 1 to day 7 of nitrogen deprivation (Supplemental Figs. S5–S7). The correlation between the increase in βC-plastoglobuli TAG and the decrease in CLD TAG after 48 h of stress, combined with their similar TAG composition, is consistent with the idea of lipid transfer from the cytoplasm into the chloroplast for the formation of βC-plastoglobuli.

A possible mechanism that may lead to a similar TAG composition of the cytoplasmatic and chloroplastic lipid droplets is a dynamic transfer of fatty acids or TAG molecules from the CLD to the βC-plastoglobuli through the chloroplast envelope membranes. This possibility is consistent with the close proximity of CLD and βC-plastoglobuli to chloroplast envelope membranes observed by electron microscopy (Fig. 12; Supplemental Figs. S5–S7). At present, we do not have any biochemical evidence for such a fatty acid or TAG transfer, but we have identified (in a proteomic analysis) lipases and acyl transferases in the CLD proteome and three PES homologs in the βC-plastoglobuli proteome, which could be involved in such a mechanism (L. Davidi, Y. Levin, S. Ben-Dor, and U. Pick, unpublished data). Such a dynamic lipid transfer may explain also why, at later stages of nitrogen deprivation/high light stress as β-carotene biosynthesis proceeds within the chloroplast, an increasing part of TAG is mobilized from the cytoplasm into the chloroplast to generate more plastoglobules for incorporation of the pigment.

In summary, we propose that, at the early stages of stress, CLD TAG is produced at the ER, mostly by incorporation of new synthesized fatty acids at the ER, and the process may involve fatty acid shuttling through PC or another polar membrane lipid. Subsequently, plastoglobuli start to be created within the chloroplast from TAG and are made, in part, from fatty acids hydrolyzed from chloroplast membrane lipids and in part, from fatty acids or TAG molecules derived from cytoplasmic droplets.

It is interesting to compare the similarities and differences between *D. bardawil* and *C. reinhardtii*: Starchless mutants of *C. reinhardtii* also accumulate lipid droplets in both the cytoplasm and the chloroplast, but the chloroplastic droplets resemble in size those droplets in the cytoplasm, do not contain β-carotene, and have not been characterized. Interestingly, the CLDs in these mutants were observed to adhere to the outer chloroplast envelope (Goodson et al., 2011) similar to the observation in *D. bardawil*. Moreover, as already discussed, the fatty acids at the *sn-2* position in *C. reinhardtii* TAGs are primarily C16, suggesting that they are made in the chloroplast by the same enzyme that produces chloroplast membrane lipids, whereas in *D. bardawil*, it is a mixed C16/C18 composition, differing from chloroplast polar lipids, indicating that most TAGs are not produced in the chloroplast.

Nevertheless, there are several clear biochemical and physiological differences between these species that could explain this difference. First, *Dunaliella* is a strict photoautotroph in contrast to *C. reinhardtii*, which is a heterotroph, and its response to nitrogen deprivation is less severe than reported in *C. reinhardtii* (Moellering and Benning, 2010; Cakmak et al., 2012; Msanne et al., 2012). Also, the nitrogen-depleted *Dunaliella* cells maintain high photosynthetic activity (50%–100% of the activity of control cells after 48 h of nitrogen deprivation on a per-cell basis). Second, *Dunaliella* contains PC (Evans et al., 1982; Fried et al., 1982; Evans and Kates, 1984; Al-Hasan et al., 1987; Peeler et al., 1989), whereas *C. reinhardtii* lacks PC (Giroud et al., 1988). Because PC is an essential component in the transfer of fatty acids between the cytoplasm and the chloroplast (Li-Beisson et al., 2010), its absence in *C. reinhardtii* may result in a different subcellular trafficking of lipids than in plants and other algae (Li et al., 2012). Third, *C. reinhardtii* does not synthesize massive amounts of β-carotene, which have to be deposited in TAG droplets, like in the case in *D. bardawil* under nitrogen deprivation. It is possible, therefore, that *D. bardawil* evolved a unique mechanism for TAG accumulation in the chloroplast to enable the deposition of β-carotene in this lipid droplets.

The finding that the polar lipid compositions in CLD and βC-plastoglobuli differ (Fig. 1C) suggests that the origins of the polar lipid monolayers of these lipid droplets are different. CLD polar lipids most probably originate in the ER. In contrast, the similarity of βC-plastoglobuli polar lipids to thylakoid/stroma membrane galactolipids (Fig. 1C) suggests that they originate from chloroplast membranes. Indeed, our electron microscopy images indicate close contacts between βC-plastoglobuli and thylakoid/inner envelope membranes (Fig. 12; Supplemental Figs. S5–S7), consistent with a dynamic exchange of polar lipids between these organelles. Similar close contacts between plant plastoglobuli and chloroplast envelope and thylakoid membranes have been previously reported (Austin et al., 2006). This finding is consistent with the suggested function of lipid droplets in interorganellar lipid transfer (Liu et al., 2007; Zehmer et al., 2009).

The βC-plastoglobuli and the CLD are characterized by different major lipid-associated proteins (Figs.

6 and 9): CGP (Katz et al., 1995) and MLDP (Davidi et al., 2012) in βC-plastoglobuli and CLD, respectively. The CGP protein, which has been previously characterized at the protein level (Katz et al., 1995), differs in sequence from green algae MLDPs, suggesting that it has a different origin.

We have shown in this work that formation of two lipid bodies in *D. bardawil* is a complex event that involves both hydrolysis of membrane lipids and de novo synthesis, and also, it probably involves transmembrane lipid transfer into the chloroplast. Although the molecular details of this mechanism are still not clear, we believe that our study and our proteomic analysis of these lipid droplets will contribute to the presently poor understanding of the biogenesis of lipid droplet in plants and microalgae.

MATERIALS AND METHODS

Strain and Growth Condition

Dunaliella bardawil is an isolated species (Ben-Amotz et al., 1989) deposited at the American Type Culture Collection (no. 30861). Culturing conditions and growth media were as previously described (Ben-Amotz et al., 1989). The media were supplemented with 2 M NaCl. To induce nitrogen limitation, midlog phase cells were centrifuged for 5 min at 5,000*g*, washed one time with growth medium lacking KNO_3 (−N medium), and resuspended in −N medium. The light intensity was raised from 150 to 300 $\mu Em^{-2} s^{-1}$ for growth in complete and nitrogen-deprived media, respectively. Cells were counted with the automated cell counter Cellometer (Nexelom Bioscience LLC).

Lipid Droplets Isolation

Isolation of lipid droplets was performed essentially as previously described with some modifications (Jiménez and Pick, 1994, Katz et al., 1995). In brief, algae after 2 d of nitrogen deprivation were washed, osmotically lyzed, and centrifuged at low speed for separation of the cytoplasmatic and chloroplastic fractions. Chloroplasts were passed two times through a 25-mL syringe (1.5 inches, 21 gauge) and centrifuged for 15 min at 5,000*g*. This treatment was found to release the majority of CLD. Chloroplasts were pelleted by centrifugation, washed two times, and lyzed by sonication. Purification of CLD and βC-plastoglobuli was performed by floatation on a discontinuous Suc gradient consisting of three layers (30% [w/v] Suc containing the droplet fraction, 15% [w/v] Suc, and 5% [w/v] Suc, all containing 10 mM Tris·HC1, pH 8) and centrifugation at 75,000*g* for 2 h. The crude lipid droplets, recovered from the top fraction, were collected and repurified by flotation on a second Suc gradient. The purified lipid droplets were collected from the top and kept frozen in liquid nitrogen.

Cloning the CGP Gene

This part of the work was performed during 1993–1995 by Tzipi Shoham and Irena Gokhman (Shoham, 1995). CGP (National Center for Biotechnology Information accession no. JX646677) was cloned from a cDNA library of high light-induced *D. bardawil* cells with the aid of anti-CGP polyclonal antibodies. In brief, *D. bardawil* culture in complete growth medium (Fisher et al., 1994) was exposed for 36 h to high light intensity of 1,600 $\mu E\ m^{-2}\ s^{-1}$ in a Warburg temperature-controlled shaker. RNA was isolated using Tri Reagent. cDNA to poly(A+) mRNA was synthesized and cloned into the γ-Uni-ZAP XR expression vector (Promega) as described (Fisher et al., 1996). A phage clone was isolated, and a screen with anti-CGP antibodies (Katz et al., 1995) was subsequently shown to include a partial 3′ end of the CGP gene. The full-length cDNA was isolated by the 5′-RACE procedure (CLONTECH Laboratories). To obtain the corresponding genomic DNA sequences, primers based on cDNA sequences were used with templates of genomic DNA digested by Sau3A, *Hae*II, *Taq*I, or *Msp*I followed by fragment circularization by ligase in several consecutive steps of inverted PCR amplification and subsequent cloning.

Generation of Anti-MLDP and Anti-CGP Antibodies

Polyclonal antibodies against CGP and MLDP were raised in rabbits as described before (Katz et al., 1995; Davidi et al., 2012).

Gel Electrophoresis and Western Analysis

Protein extracts from total cells were generated from pellets of culture samples containing 2×10^6 cells resuspended in 0.1 mL of bursting solution (5 mM HEPES [pH 7.5], 5 mM γ-caproic acid, 1 mM benzamidine, 1 mM phenylmethylsulfonyl fluoride) followed by the addition of 50 μL of SDS sample buffer. Proteins from isolated lipid droplets and pure chloroplasts (purified as described below for chloroplast fraction at 0 time point) were precipitated in 80% (v/v) acetone (Davidi et al., 2012). Proteins were analyzed by 12% (w/v) SDS-PAGE and stained with Coomassie Blue or immunoblotted with anti-MLDP, anti-CGP, or anti-Rubisco (a gift from Meir Edelmann) antibodies. Dilution factors of anti-MLDP, anti-CGP, and anti-Rubisco were 1:1,000, 1:2,000, and 1:20,000, respectively.

cDNA Preparation

Cells precultured for 48 h in complete growth medium were collected by centrifugation, washed one time, and cultured in nitrogen-deficient medium. After 0, 6, 12, 24, 32, 48, 72, 96, and 168 h, samples of 10 mL containing 1 to 2×10^7 cells were taken for RNA isolation. The cells were collected by centrifugation, immediately flash frozen in liquid nitrogen, and stored at −80°C for further use. Total RNA was isolated using the trireagent procedure according to the manufacturer's protocol (Molecular Research Center). Independent RNA isolations were conducted for each growth period. Template cDNA was synthesized using 0.1 μg of total RNA in a total volume of 20 μL using Superscript Kit (Invitrogen). MLDP and CGP gene expression of nitrogen-deprived cells was examined using MLDP gene primers (forward, 5′-GAAGCCATACTCAGGGAAC; reverse, 5′-CAGACTTTTTAAGCAACG) and CGP primers (forward, 5′-CCCCAGCAGCTGACGCCC; reverse, 5′-TGGTCAGGCACCACGGG) and compared with the expression of 18S control gene.

Bioinformatics Analysis

Sequences were routinely searched using BLAST (Altschul et al., 1997) at http://www.gravy-calculator.de/. Sequences were aligned using the CLUSTALW multiple sequence alignment program (Thompson et al., 1994) at http://www.ebi.ac.uk/Tools/msa/clustalw2/. Hydropathy plots were generated using the Kyte–Doolittle algorithm (Kyte and Doolittle, 1982) using the Prot Scale program at http://www.expasy.ch/tools/protscale.html. The value G in each graph is the GRAVY for each protein and was calculated using the GRAVY calculator program at http://www.gravy.laborfrust.de/. Post-translational modifications were screened using online software (palmitoylation, http://csspalm.biocuckoo.org/online.php; prenylation, http://mendel.imp.ac.at/sat/PrePS/index.html; nitrogen myristoylation, http://mendel.imp.ac.at/myristate/SUPLpredictor.htm; GPI-anchor, http://gpi.unibe.ch/). Secondary structure predictions were obtained using the secondary structure consensus prediction program at http://npsa-pbil.ibcp.fr/cgi-bin/npsa_automat.pl?page=/NPSA/npsa_seccons.html.

Lipid Analysis

For TAG quantification, two methods were used: Nile red fluorescence enhancement in live cells and TLC in cell extracts. Nile red was added to live cells (5×10^5 cells/mL) in the fresh growth medium or purified lipid droplets (normalized to cell concentration of 5×10^5 cells/mL) at a final concentration of 1 μM. Nile red fluorescence emission was measured after 3 to 10 min, when the signal reached maximal and steady level. The parameters of Nile red fluorescence measurement are excitation at 488 nm and emission maxima at 580 to 590 nm. The increase in fluorescence emission was used to express the relative increase in TAG level. For the TLC analysis, lipids were extracted from 10^7 cells as previously described (Khozin-Goldberg et al., 2005) and separated on TLC Silica gel 60 aluminum sheets (Merck) in *n*-hexane:diethyl-ether: acetate (85:15:1) solution. PC was isolated from microsomal membrane lipid extracts by separation on TLC plates developed vertically in chlorophorm: methanol:water (65:25:4) and horizontally in chlorophorm:methanol:isopropylamine:ammonium hydroxide (65:35:0.5:5).

Finally, lipid detection was performed by 5 min exposure to iodine vapor. For quantification, densitometric analysis of spots was compared with standards of 0.5 to 2 μg of triolein. For polar lipids detection, TLC was performed as described, with the exception that lipids were separated on chloroform: methanol:distilled deionized water (DDW; 65:25:4) with 1 μg of diacylglycerol as standard. For glactolipid detection, TLC plates were sprayed with 0.5% (w/v) α-naphtol in 50% (v/v) methanol (in DDW) and then 95% (v/v) sulfuric acid, and they were heated for 20 min at 110°C. Galactolipids appear as purple spots, whereas other polar lipids appear as yellow spots.

Chlorophyll and carotenoid contents of *D. bardawil* control and nitrogen-deprived cells or of purified lipid droplets were determined in lipid extracts from the absorbance at 663 and 480 nm, respectively (Shaish et al., 1990). For GC/MS analysis of fatty acid composition and total lipid contents, lipids were extracted from 50 mL of cells (5×10^6 cells/mL) and 2 mL of purified droplets. Total FAMEs were prepared through acid hydrolysis in methanol and then analyzed by GC/MS (Bigogno et al., 2002; performed by Inna Khozin-Goldberg in the laboratory of Zvi Cohen at Ben-Gurion University). Three replicates for each sample were examined.

The *sn*-1+3 and *sn*-2 distributions of fatty acids in TAG from purified lipid droplets were determined using Rhizopus lipase (Sigma) as previously described (Fischer et al., 1973) with minor modifications. The TAGs were extracted and separated on TLC as described above. The band containing the TAG was scraped off, dissolved in *n*-hexane, and dried. Tris·HCl buffer (40 mM, pH 7.2; 0.1 mL) containing 50 mM sodium borate (to reduce positional migration of fatty acids) was added to the dried lipid sample, and the mixture was sonicated for 10 min; 100 μL of lipase (100 units) was added to the mixture and incubated at room temperature for 10 min with continuous shaking. The reaction was terminated by the addition of 1 mL of methanol, and lipids were extracted with methanol:chloroform:DDW (1:1:1). The lipids were resolved into free fatty acids and monoacylglycerol by TLC in *n*-hexane:diethylether (20:80), and after visualizing the lipids with iodine, the free fatty acid and monoacylglycerol bands were scraped off and extracted with chloroform: methanol (1:1, v/v). FAMEs were prepared through acid hydrolysis in methanol and then analyzed by GC/MS (performed by Inna Khozin-Goldberg in the laboratory of Zvi Cohen at Ben-Gurion University). Three replicates of each sample were examined.

The *sn*-1 and *sn*-2 of microsomal and chloroplast membrane lipids were determined by exposure to Rhizopus lipase or phospholipase A2 (Sigma) and analysis of release compared with total fatty acids. Microsomal and chloroplast membranes were isolated as previously described (Jiménez and Pick, 1994; Bates et al., 2009). Tris·HCl buffer (40 mM, pH 7.2; 900 μL) and diethylether (1.5 mL) were added to the samples together with 20 μL of enzyme for 30-min incubation with shaking in room temperature. The reaction ended by evaporation of the diethylether. Lipids were extracted and separated, and fatty acids were analyzed as described above.

Cytoplasmatic and Chloroplast TAG Pools Analysis

For TAG pools analysis, *D. bardawil* cells were grown at high light in nitrogen-deficient medium, and samples were collected at 0, 12, 24, 48, 72, and 144 h. The cells were washed and lysed osmotically followed by syringe treatment and centrifugation to separate cytoplasmatic and βC-plastoglobuli lipid droplets. The supernatant was separated as cytoplasmatic fraction. The chloroplasts were washed and collected as chloroplast fraction. Both fractions were subjected to lipid extraction, and the lipids were analyzed by TLC as described above. Three repeats were made for each sample.

Incorporation of ^{14}C-PA into *D. bardawil* Lipids

To estimate the distribution of ^{14}C in the different fractions, two protocols were used. In one protocol, 5 μCi ^{14}C-PA (1 μM final concentration) was added to 300 mL *D. bardawil* culture that has been induced for 12 h in high light at nitrogen-deficient medium. After 4 h, the cells were washed and diluted into fresh nitrogen-deprived medium supplemented with 250 μM unlabeled PA. Samples were collected after 0, 24, 48, or 72 h (total 16, 40, 64, or 88 h of nitrogen deprivation, respectively). Cytoplasmatic and chloroplastic TAGs were separated as described above. In the second protocol, cells were labeled for 5 h in complete (nitrogen-sufficient) medium before transfer to nitrogen deprivation. The incubation with ^{14}C-PA was terminated by washing and dilution with 250-fold unlabeled PA, and the cell were transferred for 48 h to nitrogen deprivation at high light. Cell samples were taken before and 48 h after nitrogen deprivation for lysis and fractionation into cytoplasmic membranes, chloroplast membranes, cytoplasmic droplets, and βC-plastoglobuli as described above; ^{14}C in each fraction was counted. The extracted lipids from each fraction were also separated on TLC (as described above), and the TAG bands were scraped off and dissolved in 1 mL of *n*-hexane and 10 mL of scintillation solution. The ^{14}C radiolabeling was measured using a Tricarb liquid scintillation counter (PerkinElmer).

Lipid Analysis by HPLC

The lipid profile of *D. bardawil*-purified lipid droplets was determined by reverse-phase HPLC (Waters e2695; Waters Corporation) using a 2.7-μm Halo C8 4.6- × 150-mm column (Advanced Materials Technology). For Tag analysis, the lipid extracts were dissolved in acetonitrile:isopropanol:hexane (2:2:1) and separated with a mobile phase of acetonitrile:isopropanol gradient (0%–30%) at a flow rate of 1.2 mL/min at 40°C. For fatty acid analysis, the lipid extracts were dissolved in chloroform:methanol (1:1) and separated with a mobile phase methanol:water:acetic acid (75:25:1) to acetonitrile:methanol: tetrahidrofuran:acetic acid (50:37.5:12.5:1) gradient (0%–30%) at flow rate of 0.8 mL/min at 40°C.

The lipids were detected using Corona Charged Aerosol Detector (ESA Biosciences Inc.). TAGs were identified and quantified by comparison with TAG standards: glyceryltrimyristilate (C14:0), glyceryltripalmitin (C16:0), glyceryltripalmitolein (C16:1), glyceryltristearate (C18:0), glyceryltriolein (C18:1; Sigma-Aldrich).

β-Carotene and phytoene were detected using the same system with a photodiode array detector (Waters Corp.) and identified by their absorbance spectra at 488 and 286 nm, respectively.

Electron Microscopic Techniques

Gold Immunolabeling

Samples were prepared according to the method by Tokuyasu (1973). In brief, algae cultured for 0, 1, or 6 d in nitrogen-deprived medium were fixed in 2% (w/v) glutaraldehyde and 0.1% (w/v) acroleine in growth medium for 1 h. Fixed cells were washed in growth medium and embedded in 10% (w/v) gelatin in water. The gelatin was hardened at 4°C, postfixed overnight with the fixation medium described above, washed in cacodylate buffer, and cut into 0.5-mm pieces. The embedded cell pieces were then incubated overnight in 2.3 M Suc, frozen in liquid nitrogen, and cut into 80- to 90-nm slices with an EM FC6 cryoultramicrotome (Leica Microsystems). After 30 min incubation in blocking solution (0.5% [w/v] gelatin, 0.5% [w/v] bovine serum albumin, 0.2% [w/v] Gly, and 0.1% [w/v] Tween 20 in phosphate-buffered saline [PBS]), slices were incubated for 2 h with anti-MLDP or anti-CGP polyclonal rabbit antibodies in blocking solution (1:150 dilution). Slices were washed with PBS containing 0.2% (w/v) Gly, incubated for 30 min in 10 nm colloidal gold-conjugated goat anti-rabbit antibodies (Electron Microscopy Sciences) diluted 1:20 in blocking solution, and washed in PBS and bidistilled water. Labeled sections were stained with 2% (w/v) uranyl acetate, embedded in methylcellulose, and observed in a Tecnai Spirit Transmission Electron Microscope (FEI) operating at 120 kV. Images were recorded using an Eagle 2K × 2K CCD camera (FEI).

Cryo-SEM

Algae cultured in either complete or nitrogen-deprived media for 48 h were centrifuged, and a drop of pellet was sandwiched between two aluminum platelets with depth of 25 μm each. The sample was then high-pressure frozen using an HPM010 high-pressure freezing machine (Bal-Tec). The frozen samples were mounted on a holder and transferred to a BAF 60 freeze-fracture device (Leica Microsystems) using a VCT 100 Vacuum Cryo-Transfer device (Leica Microsystems). After fracturing and etching at a temperature of −105°C for 5 min, samples were coated with 4 nm Pt/C by double-axis rotary shadowing. Samples were transferred to an Ultra 55 SEM (Zeiss) using a VCT 100 and observed using a secondary electrons in-lens detector at an acceleration voltage of 2 kV at a temperature of −120°C .

TEM Observation and Scanning Transmission Electron Microscopy Tomography

Algae cultured in complete or nitrogen-deprived media for 1, 2, 3, or 7 d were fixed in 2% (w/v) glutaraldehyde and 0.1% (w/v) acroleine in cacodylate

buffer for 1 h at room temperature and 15 h at 4°C. The fixed samples were centrifuged, and the pellet was embedded in 3.4% (w/v) agarose (BD), dehydrated in ethanol, and infiltrated in a series of increasing concentration of Epon (Electron Microscopy Sciences). After polymerization at 60°C, 60- to 80-nm sections were stained with uranyl acetate and lead citrate and examined in a Tecnai T12 electron microscope (FEI) operating at 120 kV. Images were recorded with an F224HD 2K × 2K CCD camera (TVIPS).

For scanning transmission electron microscopy tomography, blocks were prepared as above and sectioned to a thickness of approximately 470 nm, double stained with uranyl acetate and lead citrate, and decorated on both sides with 12 nm colloidal gold markers. Sections were imaged in scanning transmission mode using a bright-field detector (GatanInc) in a Tecnai F20 transmission electron microscope (FEI). Dual-axis tilt series were acquired at 1.5° intervals over a range of ±64° using Explore3D tomography acquisition software (FEI). Alignment and three-dimensional reconstruction were performed with the IMOD image-processing package (Kremer et al., 1996).

Supplemental Data

The following materials are available in the online version of this article.

Supplemental Figure S1. Improvement of CLD purification.

Supplemental Figure S2. Multiple sequence alignment of CGP and SOUL heme-binding protein orthologs.

Supplemental Figure S3. Hydropathy plot and secondary structure prediction of MLDP and CGP.

Supplemental Figure S4. Localization of MLDP and CGP by Gold immunolabeling after 1 d of N deprivation.

Supplemental Figure S5. TEM image of *D. bardawil* control and 1-d N-deprived cells.

Supplemental Figure S6. TEM image of *D. bardawil* N-deprived cells after 3 d.

Supplemental Figure S7. TEM image of *D. bardawil* N-deprived cells after 7 d.

Supplemental Table S1. Fatty acid *sn-2* and *sn-1* positional analysis of membrane lipids.

Supplemental Movie S1. Tomographic reconstruction movie of *D. bardawil* cell after 1 d of N deprivation.

Received January 1, 2014; accepted February 20, 2014; published February 24, 2014.

LITERATURE CITED

Al-Hasan RH, Ghannoum MA, Sallal AK, Abu-Elteen KH, Radwan SS (1987) Correlative changes of growth, pigmentation and lipid composition of *Dunaliella salina* in response to halostress. J Gen Microbiol **133:** 2607–2616

Altschul SF, Madden TL, Schäffer AA, Zhang J, Zhang Z, Miller W, Lipman DJ (1997) Gapped BLAST and PSI-BLAST: a new generation of protein database search programs. Nucleic Acids Res **25:** 3389–3402

Austin JR II, Frost E, Vidi PA, Kessler F, Staehelin LA (2006) Plastoglobules are lipoprotein subcompartments of the chloroplast that are permanently coupled to thylakoid membranes and contain biosynthetic enzymes. Plant Cell **18:** 1693–1703

Avron A, Ben-Amotz A (1992) *Dunaliella*: Physiology, Biochemistry and Biotechnology. CRC Press, Boca Raton, FL

Bates PD, Durrett TP, Ohlrogge JB, Pollard M (2009) Analysis of acyl fluxes through multiple pathways of triacylglycerol synthesis in developing soybean embryos. Plant Physiol **150:** 55–72

Ben-Amotz A, Katz A, Avron M (1982) Accumulation of β-carotene in halotolerant algae: purification and characterization of β-carotene-rich globules from *Dunaliella bardawil*. J Phycol **18:** 529–537

Ben-Amotz A, Lers A, Avron M (1988) Stereoisomers of beta-carotene and phytoene in the alga *Dunaliella bardawil*. Plant Physiol **86:** 1286–1291

Ben-Amotz A, Shaish A, Avron M (1989) Mode of action of the massively accumulated beta-carotene of *Dunaliella bardawil* in protecting the alga against damage by excess irradiation. Plant Physiol **91:** 1040–1043

Bigogno C, Khozin-Goldberg I, Adlerstein D, Cohen Z (2002) Biosynthesis of arachidonic acid in the oleaginous microalga Parietochloris incisa (Chlorophyceae): radiolabeling studies. Lipids **37:** 209–216

Bréhélin C, Kessler F, van Wijk KJ (2007) Plastoglobules: versatile lipoprotein particles in plastids. Trends Plant Sci **12:** 260–266

Cakmak T, Angun P, Ozkan AD, Cakmak Z, Olmez TT, Tekinay T (2012) Nitrogen and sulfur deprivation differentiate lipid accumulation targets of *Chlamydomonas reinhardtii*. Bioengineered **3:** 343–346

Capuano F, Beaudoin F, Napier JA, Shewry PR (2007) Properties and exploitation of oleosins. Biotechnol Adv **25:** 203–206

Cho S, Thompson G Jr (1987a) Metabolism of galactolipids in *Dunaliella salina*. *In* **Stumpf P, Mudd JB, Nes WD**, eds, The Metabolism, Structure, and Function of Plant Lipids. Springer, New York, pp 623–629

Cho SH, Thompson GA Jr (1987b) On the metabolic relationships between monogalactosyldiacylglycerol and digalactosyldiacylglycerol molecular species in *Dunaliella salina*. J Biol Chem **262:** 7586–7593

Davidi L, Katz A, Pick U (2012) Characterization of major lipid droplet proteins from Dunaliella. Planta **236:** 19–33

Evans R, Kates M (1984) Lipid composition of halophilic species of *Dunaliella* from the dead sea. Arch Microbiol **140:** 50–56

Evans RW, Kates M, Ginzburg M, Ginzburg BZ (1982) Lipid composition of halotolerant algae, *Dunaliella parva* lerche and *Dunaliella tertiolecta*. Biochim Biophys Acta **712:** 186–195

Fan J, Andre C, Xu C (2011) A chloroplast pathway for the de novo biosynthesis of triacylglycerol in *Chlamydomonas reinhardtii*. FEBS Lett **585:** 1985–1991

Farese RV Jr, Walther TC (2009) Lipid droplets finally get a little R-E-S-P-E-C-T. Cell **139:** 855–860

Fischer W, Heinz E, Zeus M (1973) The suitability of lipase from *Rhizopus arrhizus delemar* for analysis of fatty acid distribution in dihexosyl diglycerides, phospholipids and plant sulfolipids. Hoppe Seylers Z Physiol Chem **354:** 1115–1123

Fisher M, Gokhman I, Pick U, Zamir A (1996) A salt-resistant plasma membrane carbonic anhydrase is induced by salt in *Dunaliella salina*. J Biol Chem **271:** 17718–17723

Fisher M, Pick U, Zamir A (1994) A salt-induced 60-kilodalton plasma membrane protein plays a potential role in the extreme halotolerance of the alga *Dunaliella*. Plant Physiol **106:** 1359–1365

Frandsen GI, Mundy J, Tzen JT (2001) Oil bodies and their associated proteins, oleosin and caleosin. Physiol Plant **112:** 301–307

Fried A, Tietz A, Ben-Amotz A, Eichenberger W (1982) Lipid composition of the halotolerant alga, *Dunaliella bardawil*. Biochim Biophys Acta **713:** 419–426

Giroud C, Gerber A, Eichenberger W (1988) Lipids of *Chlamydomonas reinhardtii*. Analysis of molecular species and intracellular site(s) of biosynthesis. Plant Cell Physiol **29:** 587–595

Goodson C, Roth R, Wang ZT, Goodenough U (2011) Structural correlates of cytoplasmic and chloroplast lipid body synthesis in *Chlamydomonas reinhardtii* and stimulation of lipid body production with acetate boost. Eukaryot Cell **10:** 1592–1606

Guermeur Y, Geourjon C, Gallinari P, Deléage G (1999) Improved performance in protein secondary structure prediction by inhomogeneous score combination. Bioinformatics **15:** 413–421

Ha KS, Thompson GA (1991) Diacylglycerol metabolism in the green alga *Dunaliella salina* under osmotic stress: possible role of diacylglycerols in phospholipase C-mediated signal transduction. Plant Physiol **97:** 921–927

Häder DP, Lebert M (2009) Photoorientation in photosynthetic flagellates. Methods Mol Biol **571:** 51–65

Heinz E, Roughan PG (1983) Similarities and differences in lipid metabolism of chloroplasts isolated from 18:3 and 16:3 plants. Plant Physiol **72:** 273–279

Hsieh K, Huang AH (2004) Endoplasmic reticulum, oleosins, and oils in seeds and tapetum cells. Plant Physiol **136:** 3427–3434

Huang AH (1992) Oil bodies and oleosins in seeds. Annu Rev Plant Physiol Plant Mol Biol **43:** 177–200

Huang AH (1996) Oleosins and oil bodies in seeds and other organs. Plant Physiol **110:** 1055–1061

Huang NL, Huang MD, Chen TL, Huang AH (2013) Oleosin of subcellular lipid droplets evolved in green algae. Plant Physiol **161:** 1862–1874

James GO, Hocart CH, Hillier W, Chen H, Kordbacheh F, Price GD, Djordjevic MA (2011) Fatty acid profiling of *Chlamydomonas reinhardtii* under nitrogen deprivation. Bioresour Technol **102:** 3343–3351

Jiménez C, Pick U (1994) Differential stereoisomer compositions of β,β-carotene in thylakoids and pigment globules in *Dunaliella*. J Plant Physiol **143:** 257–263

Jin E, Polle JEW (2009) Carotenoid biosynthesis in *Dunaliella* (Chlorophyta). *In* A Ben Amotz, JEW Polle, DVS Rao, eds, The Alga Dunaliella. Science Publishers, Enfield, NH, pp 147–171

Joyard J, Ferro M, Masselon C, Seigneurin-Berny D, Salvi D, Garin J, Rolland N (2010) Chloroplast proteomics highlights the subcellular compartmentation of lipid metabolism. Prog Lipid Res **49:** 128–158

Katz A, Jimenez C, Pick U (1995) Isolation and characterization of a protein associated with carotene globules in the alga *Dunaliella bardawil*. Plant Physiol **108:** 1657–1664

Kessler F, Vidi PA (2007) Plastoglobule lipid bodies: their functions in chloroplasts and their potential for applications. Adv Biochem Eng Biotechnol **107:** 153–172

Khozin-Goldberg I, Shrestha P, Cohen Z (2005) Mobilization of arachidonyl moieties from triacylglycerols into chloroplastic lipids following recovery from nitrogen starvation of the microalga *Parietochloris incisa*. Biochim Biophys Acta **1738:** 63–71

Kim H, Huang AC (2003) Oleosins and plastid-lipid-associated proteins in Arabidopsis. *In* N Murata, M Yamada, I Nishida, H Okuyama, eds, Advanced Research on Plant Lipids. Springer, Dordrecht, The Netherlands, pp 147–150

Kreimer G (2009) The green algal eyespot apparatus: a primordial visual system and more? Curr Genet **55:** 19–43

Kremer JR, Mastronarde DN, McIntosh JR (1996) Computer visualization of three-dimensional image data using IMOD. J Struct Biol **116:** 71–76

Kyte J, Doolittle RF (1982) A simple method for displaying the hydropathic character of a protein. J Mol Biol **157:** 105–132

Li X, Moellering ER, Liu B, Johnny C, Fedewa M, Sears BB, Kuo MH, Benning C (2012) A galactoglycerolipid lipase is required for triacylglycerol accumulation and survival following nitrogen deprivation in *Chlamydomonas reinhardtii*. Plant Cell **24:** 4670–4686

Li-Beisson Y, Shorrosh B, Beisson F, Andersson MX, Arondel V, Bates PD, Baud S, Bird D, Debono A, Durrett TP, et al (2010) Acyl-lipid metabolism. Arabidopsis Book **8:** e0133

Lin IP, Jiang PL, Chen CS, Tzen JTC (2012) A unique caleosin serving as the major integral protein in oil bodies isolated from *Chlorella* sp. cells cultured with limited nitrogen. Plant Physiol Biochem **61:** 80–87

Lippold F, vom Dorp K, Abraham M, Hölzl G, Wewer V, Yilmaz JL, Lager I, Montandon C, Besagni C, Kessler F, et al (2012) Fatty acid phytyl ester synthesis in chloroplasts of *Arabidopsis*. Plant Cell **24:** 2001–2014

Liu B, Benning C (2013) Lipid metabolism in microalgae distinguishes itself. Curr Opin Biotechnol **24:** 300–309

Liu P, Bartz R, Zehmer JK, Ying YS, Zhu M, Serrero G, Anderson RGW (2007) Rab-regulated interaction of early endosomes with lipid droplets. Biochim Biophys Acta **1773:** 784–793

Liu TH, Chyan CL, Li FY, Tzen JT (2009) Stability of artificial oil bodies constituted with recombinant caleosins. J Agric Food Chem **57:** 2308–2313

Lundquist PK, Poliakov A, Bhuiyan NH, Zybailov B, Sun Q, van Wijk KJ (2012) The functional network of the Arabidopsis plastoglobule proteome based on quantitative proteomics and genome-wide coexpression analysis. Plant Physiol **158:** 1172–1192

Moellering ER, Benning C (2010) RNA interference silencing of a major lipid droplet protein affects lipid droplet size in *Chlamydomonas reinhardtii*. Eukaryot Cell **9:** 97–106

Msanne J, Xu D, Konda AR, Casas-Mollano JA, Awada T, Cahoon EB, Cerutti H (2012) Metabolic and gene expression changes triggered by nitrogen deprivation in the photoautotrophically grown microalgae *Chlamydomonas reinhardtii* and *Coccomyxa* sp. C-169. Phytochemistry **75:** 50–59

Murphy DJ (2012) The dynamic roles of intracellular lipid droplets: from archaea to mammals. Protoplasma **249:** 541–585

Nguyen HM, Baudet M, Cuiné S, Adriano JM, Barthe D, Billon E, Bruley C, Beisson F, Peltier G, Ferro M, et al (2011) Proteomic profiling of oil bodies isolated from the unicellular green microalga *Chlamydomonas reinhardtii*: with focus on proteins involved in lipid metabolism. Proteomics **11:** 4266–4273

Peeler TC, Stephenson MB, Einspahr KJ, Thompson GA (1989) Lipid characterization of an enriched plasma membrane fraction of *Dunaliella salina* grown in media of varying salinity. Plant Physiol **89:** 970–976

Peled E, Leu S, Zarka A, Weiss M, Pick U, Khozin-Goldberg I, Boussiba S (2011) Isolation of a novel oil globule protein from the green alga *Haematococcus pluvialis* (Chlorophyceae). Lipids **46:** 851–861

Peled E, Pick U, Zarka A, Shimoni E, Leu S, Boussiba S (2012) Light-Induced oil globule migration in *Haematococcus pluvialis* (Chlorophyceae). J Phycol **48:** 1209–1219

Purkrtova Z, Jolivet P, Miquel M, Chardot T (2008) Structure and function of seed lipid-body-associated proteins. C R Biol **331:** 746–754

Rabbani S, Beyer P, Lintig J, Hugueney P, Kleinig H (1998) Induced β-carotene synthesis driven by triacylglycerol deposition in the unicellular alga *Dunaliella bardawil*. Plant Physiol **116:** 1239–1248

Roessler PG (1990) Environmental control of glycerolipid metabolism in microalgae: commercial implications and future research directions. J Phycol **26:** 393–399

Schmidt M, Gessner G, Luff M, Heiland I, Wagner V, Kaminski M, Geimer S, Eitzinger N, Reissenweber T, Voytsekh O, et al (2006) Proteomic analysis of the eyespot of *Chlamydomonas reinhardtii* provides novel insights into its components and tactic movements. Plant Cell **18:** 1908–1930

Shaish A, Avron M, Ben-Amotz A (1990) Effect of Inhibitors on the formation of stereoisomers in the biosynthesis of β-carotene in *Dunaliella bardawil*. Plant Cell Physiol **31:** 689–696

Shifrin NS, Chisholm SW (1981) Phytoplankton lipids: interspecific differences and effects of nitrate, silicate and light-dark cycles. J Phycol **17:** 374–384

Shoham T (1995) Cloning of a beta-carotene lipid globule-associated protein gene from the hallotolerant green alga *Dunaliella bardawil*. MSc thesis. The Weizmann Institute of Science, Rehovot, Israel

Siaut M, Cuiné S, Cagnon C, Fessler B, Nguyen M, Carrier P, Beyly A, Beisson F, Triantaphylidès C, Li-Beisson Y, et al (2011) Oil accumulation in the model green alga *Chlamydomonas reinhardtii*: characterization, variability between common laboratory strains and relationship with starch reserves. BMC Biotechnol **11:** 7

Tamura K, Peterson D, Peterson N, Stecher G, Nei M, Kumar S (2011) MEGA5: molecular evolutionary genetics analysis using maximum likelihood, evolutionary distance, and maximum parsimony methods. Mol Biol Evol **28:** 2731–2739

Thompson GA Jr (1996) Lipids and membrane function in green algae. Biochim Biophys Acta **1302:** 17–45

Thompson JD, Higgins DG, Gibson TJ (1994) CLUSTAL W: improving the sensitivity of progressive multiple sequence alignment through sequence weighting, position-specific gap penalties and weight matrix choice. Nucleic Acids Res **22:** 4673–4680

Tokuyasu KT (1973) A technique for ultracryotomy of cell suspensions and tissues. J Cell Biol **57:** 551–565

Tzen JTC (2012) Integral proteins in plant oil bodies. Int Scholarly Res Network Bot doi:10.5402/2012/173954

Vieler A, Brubaker SB, Vick B, Benning C (2012) A lipid droplet protein of *Nannochloropsis* with functions partially analogous to plant oleosins. Plant Physiol **158:** 1562–1569

Wagner V, Ullmann K, Mollwo A, Kaminski M, Mittag M, Kreimer G (2008) The phosphoproteome of a *Chlamydomonas reinhardtii* eyespot fraction includes key proteins of the light signaling pathway. Plant Physiol **146:** 772–788

Wang ZT, Ullrich N, Joo S, Waffenschmidt S, Goodenough U (2009) Algal lipid bodies: stress induction, purification, and biochemical characterization in wild-type and starchless *Chlamydomonas reinhardtii*. Eukaryot Cell **8:** 1856–1868

Ytterberg AJ, Peltier JB, van Wijk KJ (2006) Protein profiling of plastoglobules in chloroplasts and chromoplasts: a surprising site for differential accumulation of metabolic enzymes. Plant Physiol **140:** 984–997

Zehmer JK, Huang Y, Peng G, Pu J, Anderson RGW, Liu P (2009) A role for lipid droplets in inter-membrane lipid traffic. Proteomics **9:** 914–921

Zweytick D, Athenstaedt K, Daum G (2000) Intracellular lipid particles of eukaryotic cells. Biochim Biophys Acta **1469:** 101–120